2014

Development Of Polydimethylsiloxane Mixed Matrix Membrane

Emmanuel Onuminya Ogbole
North Carolina Agricultural and Technical State University

Development of Polydimethylsiloxane Mixed Matrix Membrane

Emmanuel Onuminya Ogbole

North Carolina A&T State University

A thesis submitted to the graduate faculty

in partial fulfillment of the requirements for the degree of

MASTER OF SCIENCE

Department: Chemical, Biological and Bioengineering

Major: Chemical Engineering

Major Professor: Dr. Jianzhong Lou

Greensboro, North Carolina

2014

The Graduate School
North Carolina Agricultural and Technical State University
This is to certify that the Master's Thesis of

Emmanuel Onuminya Ogbole

has met the thesis requirements of
North Carolina Agricultural and Technical State University

Greensboro, North Carolina

2014

Approved by:

Dr Jianzhong Lou Major Professor	Dr. Shamsuddin Ilias Committee Member
Dr. Leonard C. Uitenham Committee Member	Dr. Stephen B Knisley Department Chair

Dr. Sanjiv Sarin
Dean, The Graduate School

Biographical Sketch

Emmanuel Onuminya Ogbole was born on December 23, 1975, in Kaduna, Nigeria. He earned his High National Diploma (Bachelor of Science degree equivalent) in Chemical Engineering Technology in 2004 from Kaduna Polytechnic and Masters of Business Administration (MBA) in 2011 from Adamawa State University Mubi, Nigeria. In 2005, due to his passion to serve humanity, he joined Ekklesiyar Yan' Uwa A Nigeria (a charitable organization) as HIV/AIDS Coordinator and served in that capacity for four years. In 2010, he joined the Federal Polytechnic Mubi, Adamawa as Technologist and was in active service until he left Nigeria in December, 2012 to undertake graduate program in USA. In Spring semester 2013, he enrolled into the Master of Science program in Chemical Engineering at North Carolina A&T State University. While pursuing his MS degree, Emmanuel Ogbole was awarded Six Sigma Green Belt certificate on November 25, 2013 after successfully completing the course requirements; he worked as Graduate Teaching Assistant and Research Assistant of NSF CREST Bioenergy Center at North Carolina A&T State. Emmanuel will pursue his Ph.D. in Energy and Environmental Systems at North Carolina A & T State University after completing his MS program.

Dedication

To my lovely and faithful wife, Enekole Ogbole and our children (Providence and Gerald) for their supports, patience, and understanding throughout my studies and to Dr Gerald and Eleanor Roller for their overwhelming generosity towards me and my family.

Acknowledgments

I thank the Almighty God for sustaining me through the program. I am deeply grateful to my advisor, Dr Jianzhong Lou, whose insightful critiques, professional expertise, practical academic guidance and a caring heart has been instrumental to the transformation and accomplishments in my graduate research. I am thankful to Dr. Shamsuddin Ilias for his fatherly care and unwavering support to every single need I ever brought to his attention and also for his meaningful professional contributions towards the successful completion of my master's program. My esteemed appreciation goes to Dr. Leonard C. Uitenham for his treasured comments (suggestions) as one of my thesis committee members; his well taught polymer class contributed immensely to my research work. I thank Mensavi Dangbuie for been a friend and a colleague. I am also thankful to Matthew Sharpe for introducing me to all the relevant equipment I used for the synthesis of my membrane samples. I am grateful to Dr. Vishwanath Deshmane and Richard Abrokwah for their continuous technical support and for helping me to characterize my samples. I am indebted to the Department of Chemical, Biological and Bioengineering, North Carolina A&T State University for giving me the opportunity to undertake graduate education and research. I gratefully acknowledge the financial support received from the National Science Foundation, NSF grant No. HRD-1242152. My profound gratitude to Dr. Gerald and Eleanor Roller for their supports. To my Incomparable wife and children, I say THANK YOU.

Table of Contents

List of Figures

List of Tables

Abstract

Mixed matrix membranes (MMMs) were prepared from Polydimethylsiloxane (PDMS) filled with surface-treated fumed silica (SiO_2). Techniques (TGA, SEM, and FTIR) were employed to characterize the neat membrane (PDMS) and the mixed matrix SiO_2-PDMS membrane (SiO_2-PDMS). The results confirmed SiO_2-PDMS has improved thermal property over neat PDMS. Uniform dispersion of SiO_2 within the membrane was observed. Good material interaction between PDMS and fumed SiO_2 was observed. The effects of SiO_2 on the transport pattern and permeability of O_2, N_2, CO_2, and CH_4 were studied. Results showed that the presence of SiO_2 in PDMS matrix had a significant impact on N_2 transport pattern. The incorporation of SiO_2 into polymer matrix gave rise to an increase in solubility dominant flux and a corresponding decrease in the diffusivity of the gases through the MMMs as evident in the permeability trend of: $P_{CO2} > P_{CH4} > P_{O2} > P_{N2}$. 10% SiO_2-PDMS maintained stability under continuous and repeated exposure to oxygen. 10% SiO_2-PDMS exhibited both improved O_2 permeability of about 640 Barrer and O_2/N_2 selectivity of 3.42 against neat PDMS with O_2 permeability of about 520 Barrer and O_2/N_2 selectivity for O_2 over N_2 of 2.59. However, neat PDMS had a fair performance for the separation of CO_2/CH_4 gas pair with CO_2 permeability of about 3239 Barrer and selectivity of 4.16 against 10% SiO_2-PDMS with 2967 Barrer and selectivity 4.29. This confirmed that SiO_2 as nano filler in PDMS is not a suitable material for separation of CO_2/CH_4 gas pair but could be suitable for the separation of CO_2/N_2 gas pair.

CHAPTER 1

Introduction

1.1 Introduction

Membrane-based gas and vapor separation has become an important unit operation in the chemical industry during the past thirty years [1]. The energy efficiency and simplicity of membrane separation equipment make them attractive for solution of fluid-phase separation problems. The efficiency of this technology strongly depends on the selection of membrane materials, their physico-chemical properties, and the mechanism through which permeation occurs. The optimal choice of materials for ultrathin, dense gas separation membranes is much more demanding than that of other membrane processes, such as ultrafiltration or microfiltration, where pore size and pore size distribution are the key factors [1].

Applications of membrane-based gas separation technology tend to fall into three major categories:

1. Hydrogen separation from a wide variety of slower permeating supercritical components such as CO_2, CH_4, and N_2.
2. Acid gas (CO_2 and H_2S) and water separations from natural gas [2].
3. Oxygen enrichment.

The order of the various types of applications given above provides a qualitative ranking of the relative ease of performing the three types of separation. The extraordinarily small molecular size of H_2 makes it extremely permeable and easily collected as a permeant compared to the other more bulky gases. But surprisingly, it is difficult to separate H_2 from CO_2 and H_2S, although the molecules of these latter gases are clearly much larger.

Although H_2 has a high diffusivity, because of its low condensibility, it has a very low solubility in membranes [3]. Therefore, a more soluble, lower diffusivity gas such as CO_2 may have a steady-state permeability comparable to that of H_2, since the product of solubility and diffusivity determines the permeability of a component through the membrane. The reasonably high solubilities of CO_2, H_2S, and H_2O in membranes at low partial pressures, coupled with the relatively low solubility and diffusivity of the bulky methane molecule, have made possible the second type of separations. By far, the most difficult of the three types of separation shown is the last one, involving O_2 and N_2. The potential market for O_2-enriched air for medical and furnace applications is considerable. Moreover, N_2-enriched air for blanketing of fuels and stored foods to provide nontoxic, nonresidual protection from fire and oxygen-breathing pests is an interesting possibility. Unfortunately, currently available polymer membranes have only moderate selectivities to separate oxygen and nitrogen [4]. The size and shape (and hence diffusivity) of O_2 and N_2 are quite similar; moreover, the solubility of the pair in most membranes is similar. Nevertheless, due to the importance of the problem, processes have been designed that are able to produce economical supplies of O_2- and N_2-enriched air for commercial applications.

Polymeric membranes are low-cost membranes when compared to inorganic membranes and thus are widely used materials for gas separation. They have some desired mechanical property and flexibility to be processed into different modules. However, despite the advantages that polymeric membrane has over inorganic membrane, a greater implementation of polymer membranes is hindered by their intrinsic permeability and selectivity limitations. These limitations were first identified by Robeson as an upper bound trade-off between permeability and selectivity and later more fully characterized by Freeman [5]. To improve polymeric

membrane performance, a considerable research effort has focused on the modification of polymeric materials by the incorporation of inorganic micro-scaled fillers into polymers, giving rise to the concept of mixed matrix membrane [6, 7].

1.2 Research Objectives

The overall goal of this research is to develop a defect-free nano filler modulated polymer gas separation mixed matrix membrane (for production of O_2 enriched air) with essential properties and potentials for commercialization. To achieve this goal, the following objectives were set to be accomplished:

1. Research and select polymer candidate as well as functional nano-filler and suitable solvent;
2. Develop defect-free, stable, and high performing mixed matrix membranes (MMM);
3. Perform gas permeation experiments with MMM of different nano-filler compositions;
4. Study the influence of nano-filler on the performance of MMM and establish optimal MMM composition;
5. Characterize and document the fundamental microstructure of the membranes using Fourier transform infrared spectroscopy (FTIR), thermo-gravimetric and differential calorimetric analysis (TGA-DSC) and scanning electronic microscope (SEM).

1.3 Research Outline

This thesis is organized in five chapters, including introduction, Chapter 1. Literature review pertinent to this research is presented in Chapter 2. Materials used and methods used to fabricate and characterize PDMS MMM in Chapter 3. Results and discussion in Chapter 4 and finally, Chapter 5 gives the conclusions of the work.

CHAPTER 2

Literature Review

2.1 Introduction

Oxygen constitutes 21 vol.% of the air. It is one of the widely used commodity chemical in the world [8]. Oxygen produced from air separation is used in many applications worldwide such as medical devices, steel and chemical manufacturing, and most recently carbon capture on a large scale. The scale of the operation and the required purity of oxygen determine the method of separation [9]. The separation of oxygen from air is a very large business, nearly 100 million tons of oxygen are produced every year [10]. This oxygen market is believed to be expanding in the coming years because all large-scale clean energy technologies will require oxygen as a feed [11].

There are two fundamental approaches for air separation, which are cryogenic distillation and non-cryogenic process. Cryogenic distillation is typically reserved for applications that require tonnage quantity of oxygen at ultra-low-temperature. Non-cryogenic process involves the separation of air at ambient temperatures using either molecular sieve adsorbents via pressure swing adsorption (PSA), or membrane separation process using the polymeric membranes [9].

2.2 Cryogenic Air Separation

Cryogenic distillation of air is the conventional technology for producing large quantities of oxygen. This technology has been in existence since early 1900s and is still used today to produce high purity oxygen [12]. While currently tonnage quantities of oxygen (oxygen concentration ≥99%) are carried out by the cryogenic distillation process, this technology is noted to be complex, expensive and energy intensive. By cryogenic distillation, the inlet air must

be filtered, compressed and chilled to about −185 ˚C. Thereafter, the liquefied stream is distilled in large distillation towers to separate air into its component phases (78 vol.% nitrogen, 21 vol.% oxygen, 1 vol.% argon and other trace gases), according to their boiling points. The use of cryogenic distillation for oxygen supply (oxygen concentration ≥95%) in the field of oxyfuel power plant and coal gasification has meanwhile reduced the power generation efficiencies from current best practice of around 40–30% [11].

2.3 Swing Adsorption-based Systems

Swing adsorption (SA) is one of the technologies used in the production of oxygen from air separation. This technology is suitable for small to medium-scale plant (20–100 tons/day); hence, it is not applicable to large-scale (100–300 tons/day and beyond) production of oxygen, which is typically carried out by cryogenic distillation processes. Swing adsorption process seems to be the best alternative because of the matured technology, adsorbents availability as well as a low cost energy, and highly efficient gas separation system [13]. Vacuum swing adsorption (VSA), pressure swing adsorption (PSA), temperature swing adsorption (TSA) and hybrid vacuum-pressure swing adsorption (VPSA) or temperature–pressure swing adsorption (TPSA) systems are the variation of this technology. Most of these systems are relied entirely on zeolites to trap nitrogen in order to produce oxygen with purities from 90% to 95%. It is noted that the zeolites A and X are the most important component as an adsorbent in the oxygen-pressure swing adsorption (O_2-PSA) process [14].

2.4 Membrane Air Separation Technology

Gas separation using membrane technology is a dynamic and growing field. Separation of gases by membranes offer a number of benefits over other conventional gas separation technologies, such as low capital and operating costs, lower energy requirement and, generally ease of operation and fabrication, etc. Current applications of gas separation membranes include: CO_2 capture, volatile organic compound (VOC) removal, air/gas dehumidification (gas dehydration), oxygen and nitrogen enrichment, and organic vapor removal from air or nitrogen streams [5, 15].

Polymeric membranes are widely used materials for gas separation because they have some desired mechanical property and the flexibility to be processed into different modules unlike inorganic membranes. However, polymeric membrane is hindered by their intrinsic permeability and selectivity limitations. These limitations were first identified by Robeson [16] as an upper bound trade-off between permeability and selectivity and later more fully characterized by Freeman [5]. To improve polymeric membrane performance, a considerable research effort has focused on the modification of polymeric materials by the incorporation of inorganic micro-scaled fillers into polymers [6, 7].

2.4.1 Inorganic Membranes. Inorganic membranes can be classified into two major categories based on its structure: porous inorganic membranes and dense (non-porous) inorganic membranes. Microporous inorganic membranes have two different structures: symmetric and asymmetric; and include both amorphous and crystalline membranes [17]. Inorganic membranes are usually fabricated from metals, ceramics, or pyrolyzed carbon [18]. These membranes

generally exhibit far better chemical, mechanical, thermal, and pressure stabilities and much higher gas fluxes or selectivities than polymer membranes. Inorganic membranes such as ceramic membranes have ability for absolute selectivity for gas separation at about 593 ^{0}C [5]. Inorganic molecular sieves like zeolites and carbon molecular sieves possess better diffusivity selectivity than polymeric materials. The accurate size and shape discrimination resulting from the narrow pore distribution ensures superior selectivity [19]. Even with their superior selectivity and/or permeability at high temperatures and pressure when the organic-based membranes cannot operate, the major disadvantage of these membranes lies on their substantially higher cost and difficulty to scale up the membrane area without defects; especially accounting for their synthesis which involves high temperature processes and therefore, specialized equipment [20].

2.4.2 Polymer Membranes. Polymeric membranes have variety of important industrial applications of which gas separation is very important. For gas separation, the permeability and selectivity of the membrane material determines its performance and the efficiency of the gas separation process. Based on flux density and selectivity, a membrane can be classified broadly into two classes: porous and nonporous. A porous membrane is a rigid, highly voided structure with randomly distributed inter-connected pores. The separation of materials by porous membrane is mainly a function of the permeate character and membrane properties, such as the molecular size of the membrane polymer, pore-size, and pore-size distribution. A porous membrane is very similar in its structure and function to the conventional filter. In general, only those molecules that differ considerably in size can be separated effectively by microporous membranes. Porous membranes for gas separation do exhibit very high levels of flux but with

low selectivity values. Microporous membranes are characterized by the average pore diameter d, the membrane porosity, and tortuosity of the membrane [21].

Nonporous or dense membranes on the other hand have high selectivity properties but the rates of transport of gases through the medium are usually low. An important property of a nonporous dense membrane is that even permeants of similar sizes may be separated if their solubility in the membrane differs significantly. A dense membrane can be prepared by melt extrusion, where a melt is envisioned as a solution in which the polymer in both solute and solvent. In the solution-casting method, dense membranes are cast from polymer solutions prepared by dissolution of a polymer in a solvent vehicle to form a sol. This is followed by complete evaporation of the solvent after casting. Polymer membranes have gained popularity in isolating carbon dioxide from other gases. These membranes are elastomers formed from crosslinked copolymers of high molecular weights. They are prepared as thin films by extrusion or casting. They demonstrate unique permeability properties for carbon dioxide together with high selectivity towards H_2, O_2, N_2, and CH_4 [21].

2.5 Polymeric Membrane Materials

Basically there are two types of polymeric membranes widely used commercially for gas separations: glassy and rubbery polymers. Glassy polymers are rigid and glass-like and operate below their glass transition temperatures (Tg). They have low chain intrasegmental mobility and long relaxation times. Rubbery polymers on the other hand, are flexible and soft, and they operate above their Tg. They exhibit the opposite characteristics, namely high intrasegmental mobility and short relaxation times [22]. Mostly, rubbery polymers show a high permeability, but a low selectivity, whereas glassy polymers exhibit a low permeability but a high selectivity.

Glassy polymeric membranes dominate industrial membrane separations because of their high gas selectivities, along with good mechanical properties. There are few rubbery polymers other than silicone polymers, particularly polydimethylsiloxane (PDMS), which can be used in gas separations. Glassy polymers such as polyacetylenes, poly[1-(trimethylsilyl)-1-propyne] (PTMSP), polyimides, polyamides, polyarylates, polycarbonates, polysulfones, cellulose acetate, and poly(phenylene oxide) polymers are extensively studied as polymeric materials for gas separations [23].

2.6 Mixed Matrix Membrane (MMM)

Robeson predicted an upper limit for the performance of polymeric membranes in gas separation in early 1990 [24]. Figure 1 shows the performance of various membrane materials available for the separation of O_2/N_2. The figure presents O_2 permeability (Barrer) on the horizontal axis and the membrane selectivity for O_2 over N_2 on the vertical axis (both on a logarithmic scale). For the polymeric materials, a rather general trade-off exists between permeability and selectivity, with an ‘‘upper-bound’’ evident in Figure 1. When materials with separation properties near this limit were modified based on the traditional structure– property relation, the resultant polymers have permeability and selectivity tracking along this line instead of exceeding it. On the other hand, as shown on Figure 1, the inorganic materials have properties lying far beyond the upper-bound limit for the organic polymers [25]. Though tremendous improvements had been achieved in tailoring polymer structure to enhance separation properties during the last two decades, further progress exceeding the trade-off line seems to present a severe challenge in the near future. Likewise, the application of inorganic membranes is still seriously hindered by the lack of technology to form continuous and defect-free membranes, the

extremely high cost for the membrane production, and handling issues (e.g., inherent brittleness) [26]. In view of this challenge (limitations of inorganic and organic membranes), a new approach is needed to provide an alternate and cost-effective membrane with separation properties well above the upper-bound limit between permeability and selectivity [25].

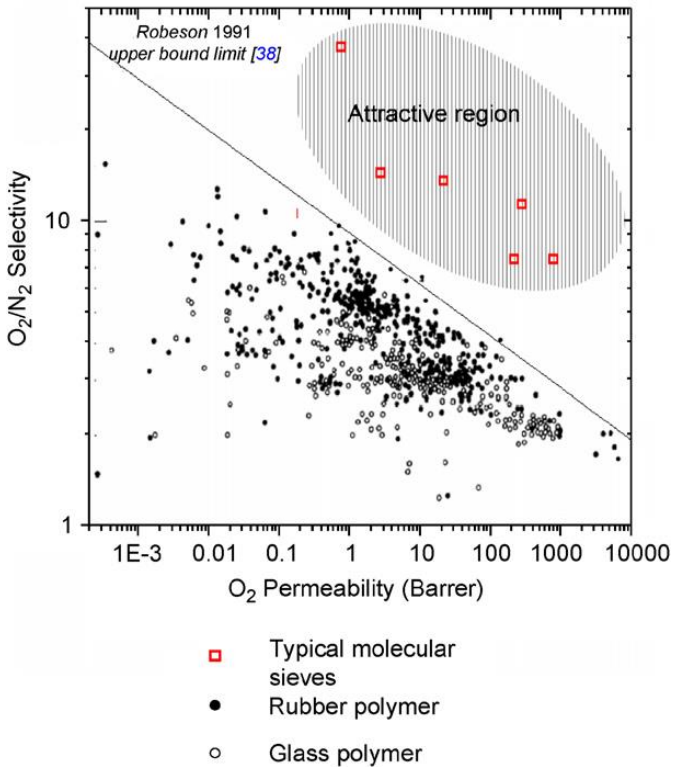

Figure 1. Membrane Performance for O_2/N_2 Gas pair Separation [24, 25].

One of the most promising approaches is the development of mixed matrix membrane. Mixed matrix membranes are normally defined as the incorporation of a solid (nano particles) into polymer matrix. The solid (dispersed) phase is the inorganic nano-scaled particles while the continuous phase is the polymer matrix [27]. Proper incorporation of the nano-scaled particles into a suitable continuous phase usually alters the molecular packing of the polymer and could result in membrane with higher selectivity, permeability, or both. At the same time, the fragility

inherent in the inorganic membranes may be avoided by using a flexible polymer as the continuous matrix [25]. The investigation of MMMs for gas separation was first reported in 1970s with the discovery of a diffusion time lag effect for CO_2 and CH_4 when adding 5Å zeolite into rubbery polymer polydimethylsiloxane (PDMS) [27]. In this work, Paul and Kemp found that the addition of 5A into the polymer matrix caused very large increases in the diffusion time lag but had only minor effects on the steady-state permeation.

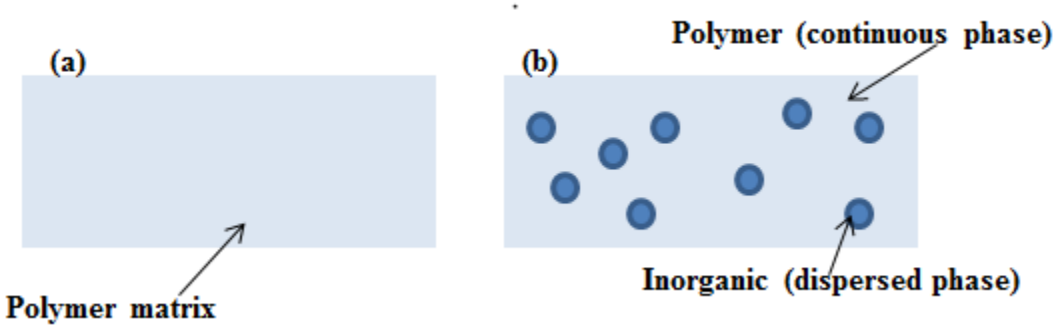

Figure 2. Schematic of: (a) Neat polymer and (b) Mixed Matrix Membrane (MMM)

2.6.1 The effects of inorganic particles on membrane performance. The addition of inorganic fillers into polymer matrix can significantly alter the transport patterns of one or several gases through the MMM when compared to that of neat polymeric matrix. The gas transport can be enhanced in several ways. First, the incorporated filler particles could change the properties of the polymer, which in turn will favor the overall transport of the penetrant gas [28]. This effect is mainly significant for particles that are well dispersed within the polymer matrix, where the fractional free volume can be greatly modified [29]. Second, the presence of filler particles may alter the molecular packing of the polymer chains near its surface, and impart great effect on the transport of large penetrates relative to small ones. Therefore, the noticeable

effect on selectivity of the gas pair involving gases with significant size difference like CO_2/He can be observed [28]. Third, the filler may act as physical crosslinker to reduce the chain segment mobility, thus increasing Tg and selectivity [30].

The interface between the inorganic particles (dispersed phase) and the polymer matrix (continuous phase) could determine the path to be passed through by one of the penetrant gases over the others [31]. This characteristics allows the selective transport of certain gases hence improved selectivity is expected, or in some cases, it can also result in increased permeability by reducing the path length of the permeate molecules.

The effect of the inorganic dispersed phase on the mixed matrix membrane properties is related to its chemical structure, surface chemistry and the type of particles; inorganic particles used for MMMs can be classified into porous and nonporous fillers [25]. For porous filler materials, the shape and size of the pores can control sorptive selectivity of the favored permeating species. The best established example of porous materials with this sieving characteristic is the micro-scaled alumino-silicate zeolites and carbon molecular sieve that have been traditionally featured by their intrinsically high separation capacities. In fact, the formation and gas separation properties of MMM using these conventional inorganic fillers have been well documented [25, 28, 32]. Nano-scaled fillers, such as silica, carbon nano tubes (CNTs) and layered silicate clay are typically characterized by intrinsically low separation capacities, In spite of that, a larger interfacial area between the fillers and the polymer matrix per unit volume of the fillers can be achieved and these have of recent attracted great attention due to their superior permeation properties [33]. The variation in the properties of these fillers have different effect may in the separation performance of the resulting MMM [28]. Porous and nonporous fillers

each has different effect on the mixed matrix membrane and can be related to their structure and their pore size.

2.6.2 Effect of porous inorganic materials. Porous fillers usually act as molecular sieving agents in the polymer matrix and separate gas molecules by their shape or size. Due to their concise apertures, porous inorganic particles usually exhibit high permeability and selectivity which is above the Robeson upper bound [34]. Therefore when these highly selective porous fillers are added to the polymer matrix, they selectively allow the desired component to pass through the pores and thus a mixed matrix membrane, whose permselectivity is higher than that of the neat polymeric membrane, can be obtained. In other words, addition of suitable porous inorganic fillers to a suitable polymer matrix not only increases the permeability of the desired component but also increases the overall selectivity of the desired component relative to the undesired component. That is, addition of porous fillers to the polymer matrix is an ideal way to overcome the traditional permeability-selectivity tradeoff of the polymeric membranes. The improvement of membrane performance due to addition of porous fillers into polymer matrix holds only when a defect free membrane is fabricated [35].

Besides the molecular sieving mechanism, adding rigid materials with large pore sizes (the materials with pore dimensions much larger than the penetrants) into the polymer matrix can induce selective surface flow of special components in the pores of the particles. In this case the more condensable or adsorbable component can adsorb and diffuse selectively through the particles and thus the less adsorbable component permeates more slowly [36]. Consequently, when feed gas mixture includes condensable components, selective surface flow must be considered. For example, in hydrocarbon drying and air drying, because of the presence of condensable and small water vapor molecule in the feed, and in dew point adjustment of natural

gas, because of the insufficient size difference between the feed gas components, a combination of surface flow and molecular sieving mechanisms may occur. While in the separation of nitrogen from hydrocarbon mixtures, hydrocarbons from air, H_2S from CH_4 and CO_2 from N_2 or CH_4, the selective surface flow can be considered as the major mechanism for transport of the condensable components through the membrane which is filled with large pore size particles [35, 36].

2.6.3 Effect of inorganic nonporous materials. Unlike porous particles, nonporous material fillers can improve the separation properties of the resultant mixed matrix membranes by increasing the matrix tortuous pattern and decreasing the diffusion of the larger molecules [37]. Also nonporous inorganic materials may disrupt the polymer chain packing and increase the free volume between polymer chains and thus increase gas diffusion. For example, Ahn et al. [38] showed that with addition of 20 vol.% nonporous silica particles into the polysulfone matrix, the void volume increases from nearly 0.2% to 2.8%. This small increase in void volume along with the insufficient polymer chain packing causes an increase in the total free volume. The increase in free volume increases the diffusion and solubility coefficients of the silica filled polymer and causes an increase in the permeability of the penetrants, as proved by Ahn et al. for all test gases (H_2, He, O_2, CO_2, N_2 and CH_4). For example, they reported that with addition of 20 vol.% silica to the polysulfone matrix, the CO_2 and CH_4 permeabilities increase by 212% (from 6.3 to 19.7 Barrer) and 400% (from 0.22 to 1.10 Barrer), respectively [38]. The hydroxyl and other functional groups on the surface of these nanomaterials may also interact with polar gases (CO_2 and SO_2) and thus improve the penetrant solubility in the resulting mixed matrix membranes [39].

2.6.4 Material selection for MMM. Suitable material selection for both the matrix and the inorganic phase is key to developing a defect-free MMM. Polymer properties as well as inorganic phase properties can affect mixed matrix membranes morphology and separation performance [25]. Usually highly selective polymers can result in mixed matrix membranes with better separation performance. For instance, glassy polymers with superior gas selectivity are preferred to highly permeable but poorly selective rubbery polymers [40]. Though, glassy polymers are better than rubbery polymers, but because of their rigid structure, poor adhesion between the polymer phase and the external surface of the particles is a major problem when used in the preparation of mixed matrix membranes [41].

Therefore, in the selection of the matrix phase, gas separation properties and the compatibility between the two phases must be considered. Zeolites and carbon molecular sieves (CMS) are the most commonly used porous inorganic fillers for mixed matrix membrane development[34]. These materials have hydrophobic internal surfaces and are being used in industry to separate air by adsorption of oxygen and to remove carbon dioxide from landfill gases. Other porous inorganic fillers used as dispersed phase in MMM are metal organic frameworks, activated carbon and carbon nanotubes [41]. When a porous material is used as filler in the polymer matrix, its pore size distribution, surface chemistry and functional groups must be consistent with the gas molecules pairs. For example, activated carbon is suitable for carbon dioxide/methane separation because it has a higher adsorption selectivity for CO_2 (polar gas) than for CH_4 (non-polar compound) but this filler is not suitable for oxygen/nitrogen separation [41].

The effect of the nonporous inorganic material on MMM separation potential is different from porous inorganic materials with sieving function; interaction between polymer-chain

segments and nanofillers as well as functional groups on the surface of the inorganic phase must be factored in material selection [39]. When silica was incorporated into a polyimide matrix, the polymer chain packing was altered, resulting to increased oxygen and nitrogen permeation rates [42]. Also, adding TiO_2 to the polyimide matrix can increase the CO_2/CH_4 and H_2/CH_4 selectivity because interactions of CO_2 and H_2 with TiO_2 are stronger than TiO_2–CH_4 interactions. Silica, TiO_2 and fullerene (C60) are the most common impermeable inorganic particles used for nanocomposite mixed matrix membrane development [43].

2.6.5 Polydimethylsiloxane (PDMS) MMM. The development of a defect-free MMM with the desired properties and enhanced membrane performance depends on the proper selection of the polymer and filler materials, their structural and physiochemical properties, and the ratios of their concentrations [44]. One of the favorable base polymers that is commonly used for developing MMMs for gas separation is PDMS [45]. Figure. 3 (PDMS structure) shows an unusual combination of an inorganic chain similar to silicates, associated with high surface energy, and organic methyl side groups, with low surface energy. The Si-O-Si linkages result in good thermal stability, low chemical reactivity and significant resistance to oxygen, ozone and UV light. On the other hand, PDMS exhibits very poor mechanical properties at room temperature as a consequence of low intermolecular forces between polymer chains, and it has a very low *T*g (−123°C) [46, 47]. PDMS has been widely used for MMM applications due to its ideal properties, which include low cost, biocompatibility, nontoxicity, and ease of fabrication.

PDMS offers one of the highest permeability coefficients for a wide range of gas species and it provides a very modest selectivity[16]. This creates the opportunity to utilize fillers to provide enhanced selectivity of PDMS to target gasses.

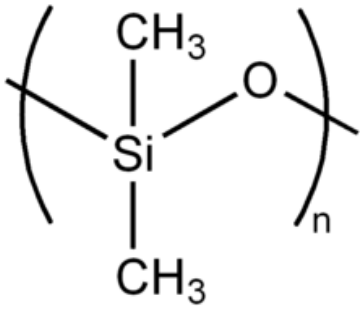

Figure 3. Chemical Structure of PDMS

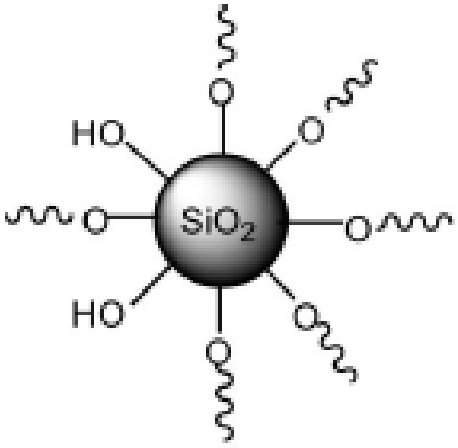

Figure 4. Fumed Silica [48]

2.6.6 Fumed silica. Intensive research in silica/polymer MMM system have shown that the addition of non-porous nanosized fumed silica (which has opposed properties with porous inorganic fillers) has great potential to affect polymer chain packing and high free- volume, which consequently bring about alteration in the gas separation properties of the resultant membrane. Due to the non-permeability of the nonporous silica particles, the addition of this filler into the polymer matrix does not directly contribute to the change of transport property, but it alters the molecular packing of the polymer chains, resulting in an improvement of the permeation as well as the selectivity [28]. Addition off nano-fumed silica into polymer matrix can give rise to two outcomes: (i) increase of polymer free volume without creating non-selective voids which in turn results in increased gas permeation properties and (ii) formation of free volume elements that are large enough to permit non-selective Knudsen transport hence resulting in a decrease in selectivity [49]. Also, the presence of silica particles is reported to induce the morphology change at the interface resulting in the increased amorphous region of the MMM as well as giving rise to increased mean distance between the polymer chains through the

reduction of the polymer chain packing density at the interface between the two phases. In such case, the polymer structure stiffness ascribed to the increased tortuosity and restricted segmental motion has resulted in higher diffusivity and diffusivity selectivity by disrupting inter-chained packing. An increasing polymer backbone stiffness, likewise plays a more determining role in the polymer separation performance in comparison with the solubility factor [50].

2.7 Transport Mechanism of Gases through Dense Membrane

The transport of gas molecules through polymer membrane and the ability of the membrane to separate gas mixtures were observed and described analytically over a century ago. Graham suggested that permeation of a penetrant molecule through a dense (i.e. nonporous) polymer membrane proceeded by a three step solution-diffusion mechanism. In this model, penetrant molecules first dissolve into the high pressure (upstream) face of the membrane, diffuse across the membrane to the low pressure (downstream) side, and desorb (or evaporate) from this face. Membrane materials currently used in gas separation applications are understood to permeate and separate small molecules based on this mechanism [51].

According to the solution-diffusion model, the permeation of gas molecules through membranes is controlled by two major parameters: diffusivity coefficient (D) and solubility coefficient (S). The diffusivity is a measure of the mobility of individual molecule passing through the voids between the polymeric chains in a membrane material. The solubility coefficient equals the ratio of the dissolved penetrant concentration in the upstream face of the polymer to the upstream penetrant partial pressure. The permeability (P) representing the ability of molecules to pass through a membrane is defined as

$$P = DS \qquad (1)$$

The ability of a membrane to separate two molecules, for example, A and B, is the ratio of their permeabilities, called the membrane selectivity,

$$\alpha_{AB} = P_A/P_B \quad (2)$$

Since P is the product of D and S, Eq. (2) may be rewritten as

$$\alpha_{AB} = (D_A/D_B)\,(S_A/S_B) \quad (3)$$

Therefore, the difference in permeability is resulted not only from diffusivity (mobility) difference of the various gas species, but also from difference in the physicochemical interactions of these species with the polymer that determine the amount that can be accommodated per unit volume of the polymer matrix [52]. The balance between the solubility selectivity and the diffusivity selectivity determines the selective transport of the component in a feed mixture. Research related to the development of polymers membranes with improved gas separation performance focuses on manipulation of penetrant diffusion coefficient via systematic modification of either/both polymer chemical structure, superstructure, chemical or thermal post treatment of the membrane. Solubility selectivity may also be increased by altering polymer structure to increase the solubility of one component in a mixture [53].

2.8 Techniques for Characterization of Mixed Matrix Membrane (MMM)

There are different characterization methods used in the analysis of the chemical structure, microstructure and morphology, as well as the physical properties, of mixed matrix membranes. Several of these techniques are specific for characterization of particular properties

of nanocomposites, and the properties of nanocomposites are also discussed correspondingly. To fully understand structure-property relationships, several characterization techniques are often employed [48]. The properties of the nanocomposites strongly depend on their composition, the size of the particles, interfacial interaction, etc. [54]. The interfacial interaction between polymer and silica (which depends on the preparative procedure) strongly affects the mechanical, thermal, and other properties of the nanocomposites. The internal surfaces (interfaces) are critical in determining the properties of nanofilled materials since silica nanoparticles have high surface area-to-volume ratio, particularly when the size decreases below 100 nm.

This high surface area-to-volume ratio means that for the same particle loading, nanocomposites will have a much greater interfacial area than microcomposites. This interfacial area leads to a significant volume fraction of polymer surrounding the particle that is affected by the particle surface and has properties different from the bulk polymer (interaction zone). Since this interaction zone is much more extensive for nanocomposites than for microcomposites, it can have significant impact on properties [55].

2.8.1 Chemical structure - Fourier transform infrared (FTIR). FTIR is used for the analysis of polymer/silica nanocomposites chemical structure. FTIR spectrometry is widely used to show the formation of nanocomposites especially for those prepared by the sol-gel reaction, in which process a silica network can be formed. The major peak at about 1100 cm^{-1} (varying with different samples in the range of 1000-1200 cm^{-1}) that is attributed to the asymmetric stretching vibrations of Si-O-Si bonds of silica can be found in the hybrids. If the condensation reaction is not complete, Si-OH groups will also exist. FTIR spectra can also supply evidence of the existence of hydrogen bonding or covalent bonding between organic and inorganic phases [48].

Figure 5 shows FTIR spectra of SiO_2 with Si-DMS. Unmodified SiO_2 was characterized by a broad band peak between 3,000 cm^{-1} and 3,700 cm^{-1}, related to the silanol groups (Si-OH) on the SiO_2 surface. Decline in silanol peak signal was associated with the appearances of three new absorbances at 912 cm^{-1}, 2,148 cm^{-1} and 2,967 cm^{-1} which are attributable to Si-H bending near the Si-O bands, Si-H stretching and C-H asymmetric stretching, respectively [56-58].

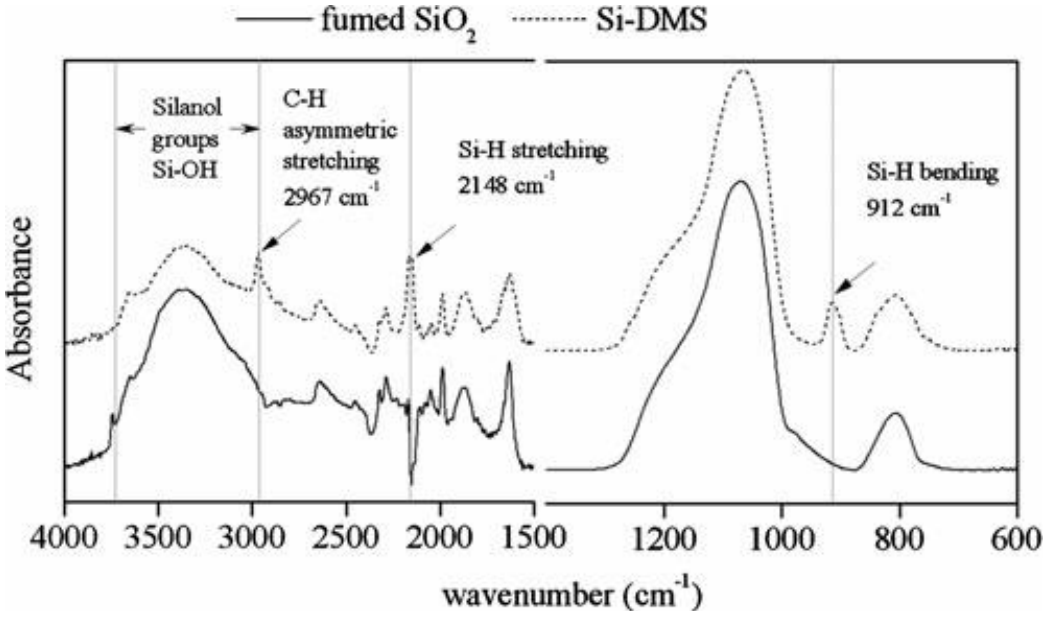

Figure 5. FTIR Spectra of the Fumed SiO_2 and Si-DMS Nanoparticles [56].

2.8.2 Microstructure - differential scanning calorimetry (DSC). Crystallization behaviors of mixed matrix membrane are usually analyzed by DSC. For PDMS-silica nanocomposite, DSC scans of the membranes samples shown in Figure 6 were used to determine the transition glass temperatures (T_g). This analysis was performed due to the sensitivity of T_g values to structural changes within the PDMS matrix. The T_g values were determined by tracing the heat flows before and after the transition, followed by obtaining the middle temperature of

the tangent line. The obtained T_g values are listed in Table 1. It is obvious that pure PDMS has lower T_g values compared to the PDMS MMMs [56].

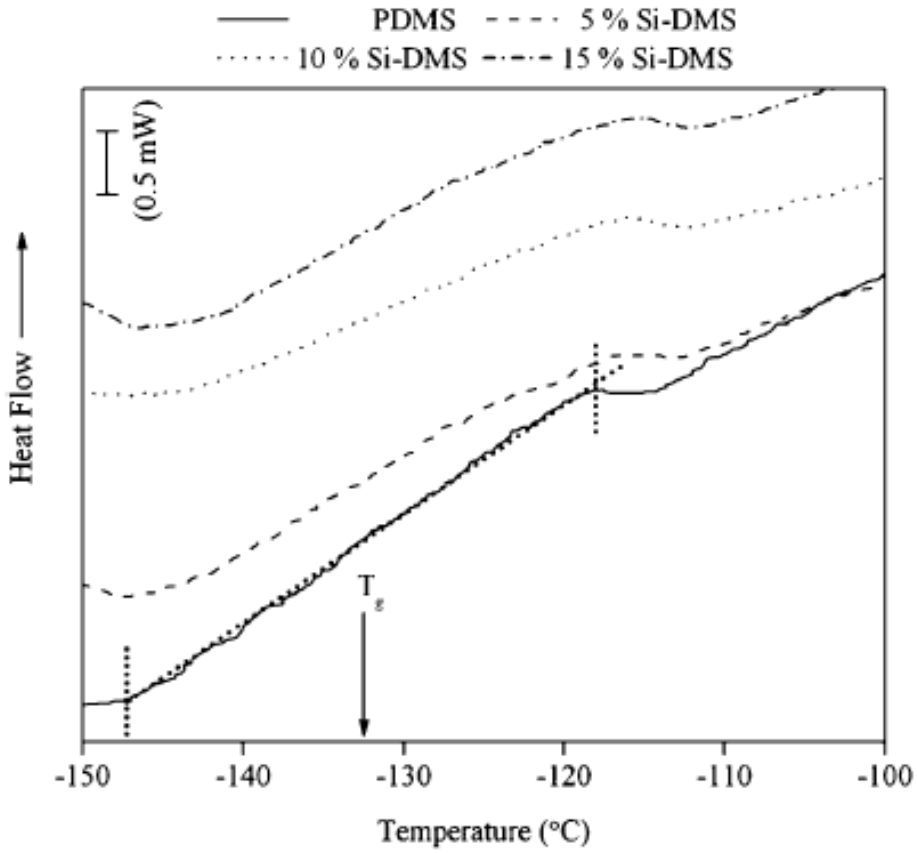

Figure 6. DSC scans of Neat PDMS and PDMS MMMs [56]

Table 1

Calculated FF and Tg Values in Neat PDMS and PDMS MMM [56].

Si-DMS (wt%)	ρ_{PDMS} in MMM (g/cm^3)	FFV	T_g(°C)
0	1.030	0.152	−132.57
5	1.026	0.155	−130.00
10	1.015	0.165	−129.73
15	1.006	0.172	−129.45

2.8.3 Morhpology –Transmission electron microscope (TEM), scanning electron microscope (SEM), and atomic force microscopy (AFM) are powerful microscopy techniques used study the morphology of nanocomposites. TEM is a microscopy technique in which a beam of electrons is transmitted through an ultra-thin specimen, interacting with the specimen as it passes through. It is difficult to receive details of some samples due to low contrast resulting from weak interaction with the electrons; this can partially be overcome by the use of stains such as phosphotungstic acid and RuO_4. At times the organic components of the sample would be decomposed by the electron beam; this can be circumvented using cryogenic microscopy (cryo-TEM), where the specimen is measured at liquid nitrogen or liquid helium temperatures in a frozen state. The recent application of electron energy loss spectroscopy imaging techniques to TEM (ESI-TEM) can provide information on the composition of polymer surfaces. This is a very useful technique for the characterization of colloidal nanocomposite particles [48]. The scanning electron microscope (SEM) is a type of electron microscope that produces images of a sample by scanning it with a focused beam of electrons. The electrons interact with atoms in the sample, producing various signals that can be detected and that contain information about the sample's surface morphology and composition. SEM images have a characteristic 3-D appearance and are therefore useful for judging the surface structure of the sample. Aside the emitted electrons, X-rays are also produced by the interaction of electrons with the sample. These can be detected in a SEM equipped for energy-dispersive X-ray (EDX) spectroscopy [48, 59]. Figure 7 shows the SEM and EDX Si-mapping photography of a PMMA/silica nanocomposite film containing 50 wt% silica. [60] From the SEM photography, aggregation of silica was not observed. The

fracture surface was very dense. Both the SEM and EDX Si-mapping results indicated the homogeneous dispersion of the silica in the polymer matrix.

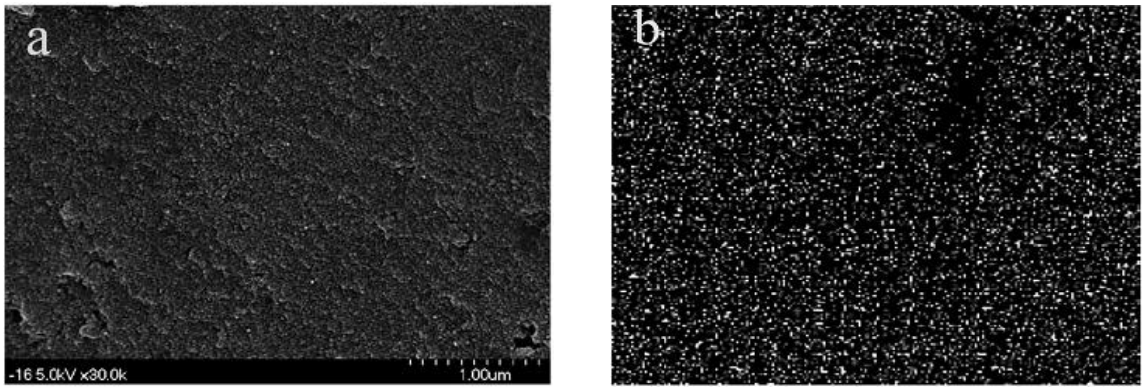

Figure 7. (a) SEM and (b) EDX-Si mapping Microphotographs of a PMMA-silica [60].

2.9 Air Separation

Membrane-based air separation is relatively new but is likely to be one of the most important since nitrogen and oxygen are the second and third most produced chemicals, respectively, in the world. In 1989, 53.8 billion pounds (24.5 billion kg) of nitrogen and 37.4 billion pounds (17.0 billion kg) of oxygen were produced [61]. Though most of this production was accomplished by cryogenic distillation of air, membrane processes are becoming increasingly attractive for smaller capacity and lower purity plants.

Membrane-based separation of nitrogen from oxygen is limited because most commercial membranes have O_2/N_2 selectivities ranging from 3.5 to 5.5 [62] . Nitrogen can be economically produced using membranes at concentrations up to 99.5% purity, but membranes are most efficient producing N_2 in the 95-98% purity range. It is difficult to produce oxygen economically

with a purity of more than 35% using membranes. Such oxygen-enrich air finds limited use in combustion processes and medical applications [62].

2.9.1 Current polymeric membrane performance in air separation. The O_2/N_2 separation remains the widely studied gas pair with more data existing

Table 2

Experimental Data Points close to the present Empirical Upper bound for O_2/N_2 [63].

Polymer	$P(O_2)$ barrers	$\alpha(O_2/N_2)$	Reference
Polyimide (BPDA-ODA)	0.079	19.8	[18]
Polyimide (BPDA-ODA)	0.170	14.2	[18]
Polyetherimide (3d: cyclohexyl	0.90	11.2	[19,20]
Polypyrrolone	1.01	10.3	[21]
Sulfonated brominated PPO	12.6	7.4	[22]
Sulfonated brominated PPO	14.0	7.0	[22]
Polyimide (BADBSBF-BTDA)	18.0	9.0	[23]
Poly[1-phenyl-2-p-	1550	2.98	[24]
PIM – 1	370	4.0	[25]
PIM – 7	190	4.5	[25]

the literature than any of the other pairs. Numerous data points show intensity just below the original upper bound with a few data points emerging above allowing for a new upper bound relationship (Figure 8). The key points defining the new upper bound are tabulated in Table 2. The position of the one data point above the present upper bound ($P(O_2)$ = 18 barrers; (O_2/N_2) = 9.0) is questioned as only one significant figure was noted for nitrogen permeability.

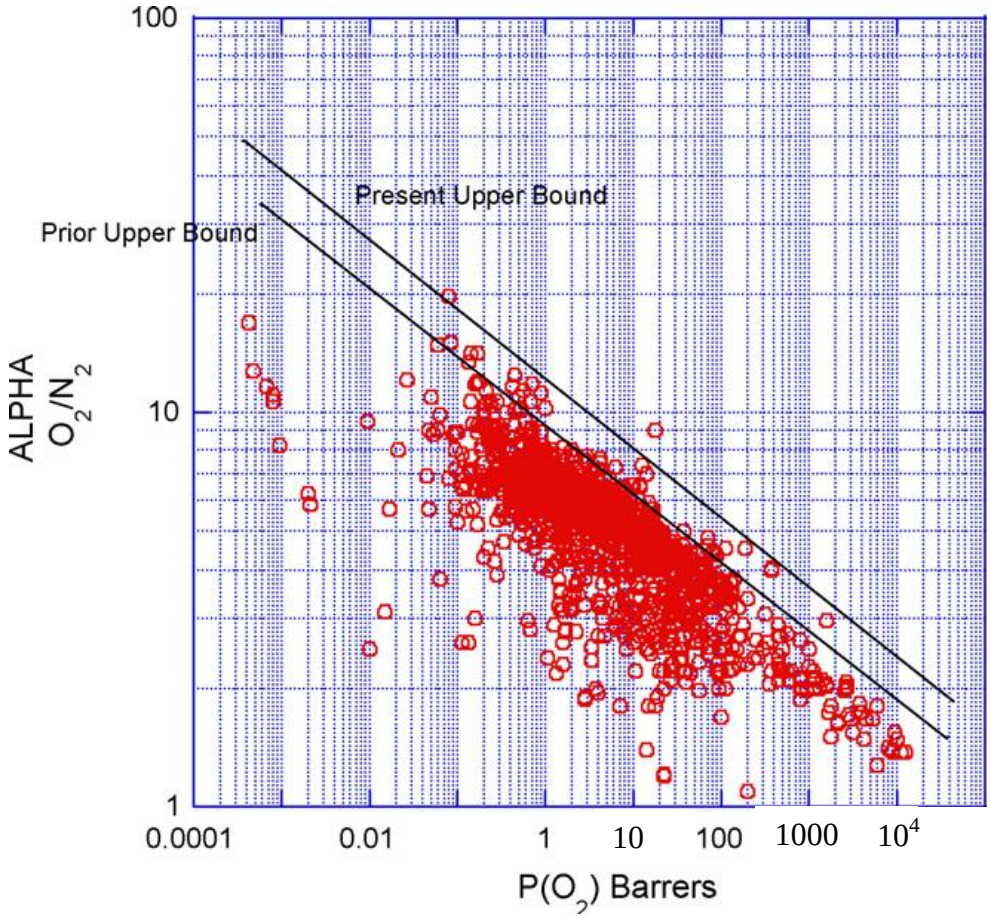

Figure 8. Upper bound Correlation for O_2/N_2 Separation [63].

Two data points (PIM-1 and PIM-7) are worth noting as these are based on ladder polymeric structures (PIM = polymers of intrinsic microporosity) thus approaching the molecular sieving type structures necessary to yield high separation capabilities. Several polyimide variants also comprise points near on the upper bound.

2.10 Applications of O_2 Enriched Air

2.10.1 Oxygen-enriched combustion. When a fuel is burned, oxygen in the combustion air chemically combines with the hydrogen and carbon in the fuel to form water and carbon dioxide, releasing heat in the process. Air is made up of 21% oxygen, 78% nitrogen, and 1% other gases. During air–fuel combustion, the chemically inert nitrogen in the air dilutes the reactive oxygen and carries away some of the energy in the hot combustion exhaust gas. An increase in oxygen in the combustion air can reduce the energy loss in the exhaust gases and increase heating system efficiency. The benefits include but not limited to:

- ***Increase efficiency*.** The flue gas heat losses are reduced because the flue gas mass decreases as it leaves the furnace. There is less nitrogen to carry heat from the furnace.
- ***Lower emissions***. Certain burners and oxy-fuel fired systems can achieve lower levels of nitrogen oxide, carbon monoxide, and hydrocarbons.
- ***Improve temperature stability and heat transfer***. Increasing the oxygen content allows more stable combustion and higher combustion temperatures that can lead to better heat transfer.
- ***Increase productivity.*** When a furnace has been converted to be oxygen enriched, throughput can be increased for the same fuel input because of higher flame temperature, increased heat transfer to the load, and reduced flue gas [64].

2.10.2 Other applications. In the chemicals and petrochemicals industries, oxygen is used as a reagent to improve the efficiency of a large number of processes. In the metallurgy and steel industries, it is also used for combustion and to adjust the carbon content of steel [65].

During combustion processes, oxygen enables to reduce the quantity of fuel used, and thus CO_2 emissions. Oxygen also lowers the formation of nitrogen oxides (NOx) that are noxious substances for both human beings and the environment. Oxygen-based combustion concentrates CO_2 into industrial fumes. This is the first step of the carbon capture and storage process.

Oxygen is also used in the process of eco-friendly paper bleaching and thus helps to avoid the use of chlorine-based substances. It also enhances the efficiency of water treatment plants by increasing biological activity.

For patients with respiratory ailments, the blood in the lungs is not able to get sufficient Oxygen. The administration of Oxygen-enriched air, otherwise known as Oxygen therapy**,** helps to improve the lives of patients who suffer from COP (Chronic Obstructive Pulmonary Disease). Oxygen is also used to treat cluster headaches, a less common and even more painful ailment than a migraine headache.

Oxygen can also sometimes be administered at pressure that exceeds atmospheric pressure, in hyperbaric chambers, for example in the treatment of Carbon monoxide poisoning or deep sea diving accidents [65].

CHAPTER 3

Materials and Method

3.1 Materials

3.1.1 Polydimethylsiloxane

PDMS was supplied by Dow Corning Corporation, USA. The specification and properties are listed in Table 3.

Table 3

PDMS (Sylgard 184 silicone elastomer) Specification

Property	Unit	Result
One or Two Part	-	Two
Color	-	Colorless
Viscosity (Base)	cP	5100
Viscosity (Mixed)	cP	3500
Thermal Conductivity	Btu/hr ft ^{0}F	0.15
Specific Gravity (Cured)	-	1.03
Working Time at 25 ^{0}C (Pot Life-hours)	hrs	1.5
Cure Time at 25 ^{0}C	hrs	48
Heat Cure Time at 100 ^{0}C	minutes	35
Heat Cure Time at 125 ^{0}C	minutes	20
Heat Cure Time at 150 ^{0}C	minutes	10
Durometer Shore	-	43
Dielectric Strength	volts/mil	500
Volume Resistivity	Ohm*cm	2.9E+14
Dissipation Factor at 100 Hz	-	0.00257
Dissipation Factor at 100 Hz	-	0.00133
Dielectric Constant 100 Hz	-	2.72
Dielectric Constant 100 Hz	-	2.68
Linear CTE (by DMA)	ppm/^{0}C	340
Tensile Strength	PSI	980
Refractive Index	@ 589 nm	1.4118
Refractive Index	@ 632.8 nm	1.4225
Refractive Index	@ 1321 nm	1.4028
Refractive Index	@ 1554	1.3997

3.1.2 Aerosil R974 (Evonik, USA) is a hydrophobic funed silica after-treated with DDS (dimethyldichlorosilane) based on a hydrophilic fumed silica with a specific surface area of $200m^2/g$

Table 4

Aerosil R974 Specification

Parameters	Specification Limits	Actual Values
BET surface area	150 - 190	157 m^2/g
pH	3.70 - 5.00	4.48
Moisture	0.5	0.30%
Carbon content	0.70 - 1.30	0.97%
Typical value of SiO_2 content is > 99.8% (based on the ignited substance		

3.1.3 Aerosil R202 (Evonik, USA) is hydrophobic fumed silica after-treated with PDMS (polydimethylsiloxane)

Table 5

Aerosil R202 Specification

Parameters	Specification Limits	Actual Values
BET surface area	80 - 120	88 m^2/g
pH	4.0 - 6.00	5.2
Moisture	0.5	0.30%
Carbon content	3.5 – 5.0	4.8%

3.2 Preparation of Membrane

The PDMS MMMs were prepared through solution casting. Required quantity of fumed silica (0, 5, 10, and 15 w% based on PDMS content) was dispersed in right amount of solvent (toluene) and stirred for 30mins and further mixed by ultrasonification for 30min to ensure

mixing at molecular level. The solvent was used to enhance even dispersion of the silica and to control the viscosity of the polymer solution. The PDMS elastomer part A was added into the

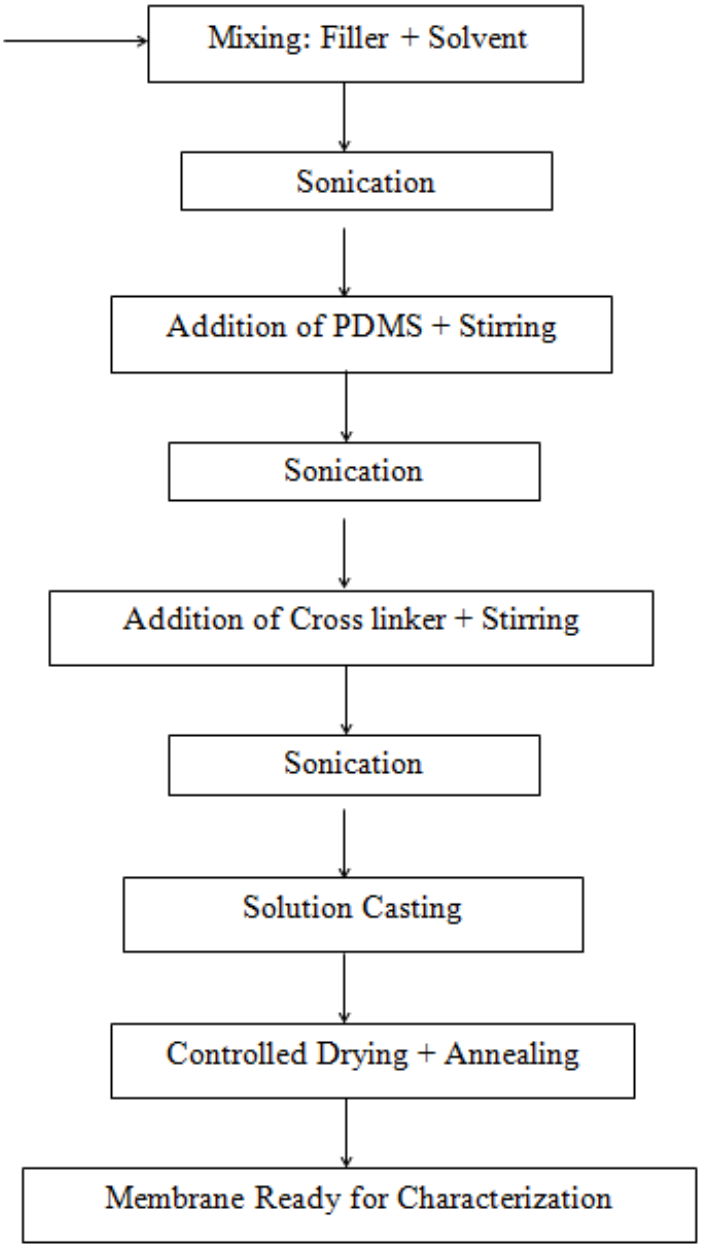

Figure 9. Laboratory Procedure for Preparing PDMS MMM

dispersion, stirred for 30min and sonicated for 30mins. Then part B of the elastomer was added into the mixture and further subjected to 30mins stirring and 60mins sonication. The PDMS MMM solution was then poured into disposable aluminium weighing dishes for 12 hrs drying at ambient condition. The samples were vacuum –dried for 24hr at room temperature. After drying, the samples were annealed under vacuum at 80^{o}C for another 24hrs. The membrane films were peeled from aluminium dishes and stored for use. Figure 9 shows the laboratory procedure developed in making PDMS MMM.

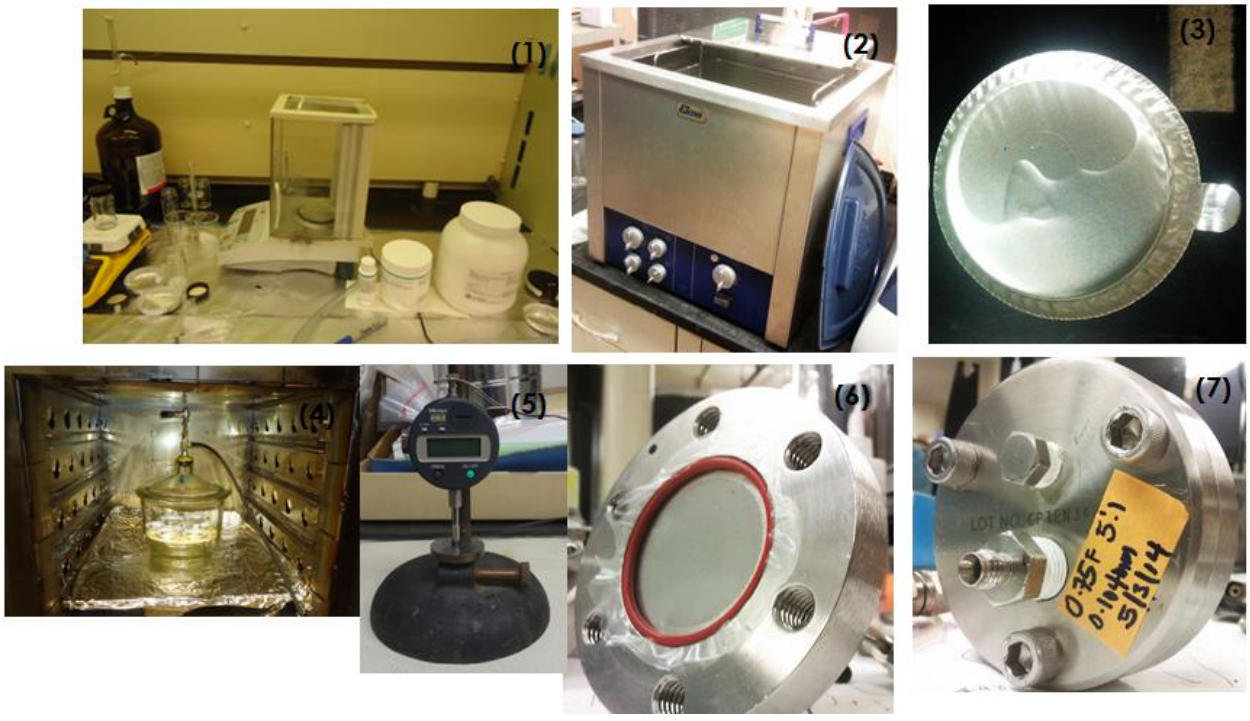

Figure 10. Pictorial Steps for Synthesis of SiO_2-PDMS

Key:

1. Fume hood for formation and mixing of polymer-silica solution
2. Water bath/sonicator for molecular dispersion of silica in polymer matrix
3. Disposable aluminium weighing dish for membrane solution casting

4. Oven for controlled vacuum drying and annealing
5. Digital micrometer for estimating membrane thickness
6. Membrane film housed in membrane cell holder
7. Loaded membrane cell holder ready for permeation test

3.3 Membrane Characterization

3.3.1 Thermal gravimetric analyzer. TGA (TA SDT Q600) was used to analyze the effects of silica on the thermal property of PDMS matrix samples under the protocol outlined below:

- Select gas 2 (air)
- Flow rate 100mL/min
- Equilibrate at 50^{o}C
- Isothermal for 30min
- Ramp 5.000^{o}C/min to 750.000^{o}C
- Isothermal for 30min
- Flow rate 0mL/min

3.3.2 Scanning electron microscope (SEM). SEM analyses of the samples were employed using Hitachi S-4800 field emission-scanning electron microscope to investigate the level of homogenous dispersion of silica in the polymer matrix**.**

3.3.3 Fourier transform infrared spectroscopy (FTIR). The FTIR spectra were recorded using Shimadzu IR Prestige-21 Fourier transform infrared (FTIR) 8300 spectrometer equipped with mercury-cadmium-telluride (MCD) detector.

3.3.4 Gas permeation tests. Pure gas permeations through PDMS MMMs were performed at different feed pressures (4.8-35 Psig), through active membrane surface area of 13.8 cm^2 at room temperature. Gas flow rates at the permeate stream were measured using bubble flow meter. Prior to measurements, the system was allowed to attain steady state condition. Permeability (P) in Barrer (10^{-10} cm^3-cm (STP)/cm^2 s cm Hg) and ideal selectivity are determined according to Eqs 3 and 4 where J is the gas flux through membrane (cm^3/cm^2 s), l is the thickness (cm) while p_1 and p_2 are the pressures (cm Hg) at the feed and permeate streams, respectively. Data generated from the pair of O_2 and N_2 and CO_2 and CH_4 permeation tests were used to plot graphs of gas flow rates (ml/min) against pressure (Psi); selectivity for O_2 over N_2 and CO_2 over CH_4 were determined from the ratio of the slopes of the graphs. The transport patterns of O_2, N_2, CO_2, and CH_4 were also gleaned and analyzed from the gas permeation tests.

$$P = \frac{J.l}{p_1 - p_2} \tag{3}$$

$$\alpha_{A/B} = \frac{P_A}{P_B} = \left(\frac{S_A}{S_B}\right)\left(\frac{D_A}{D_B}\right) \tag{4}$$

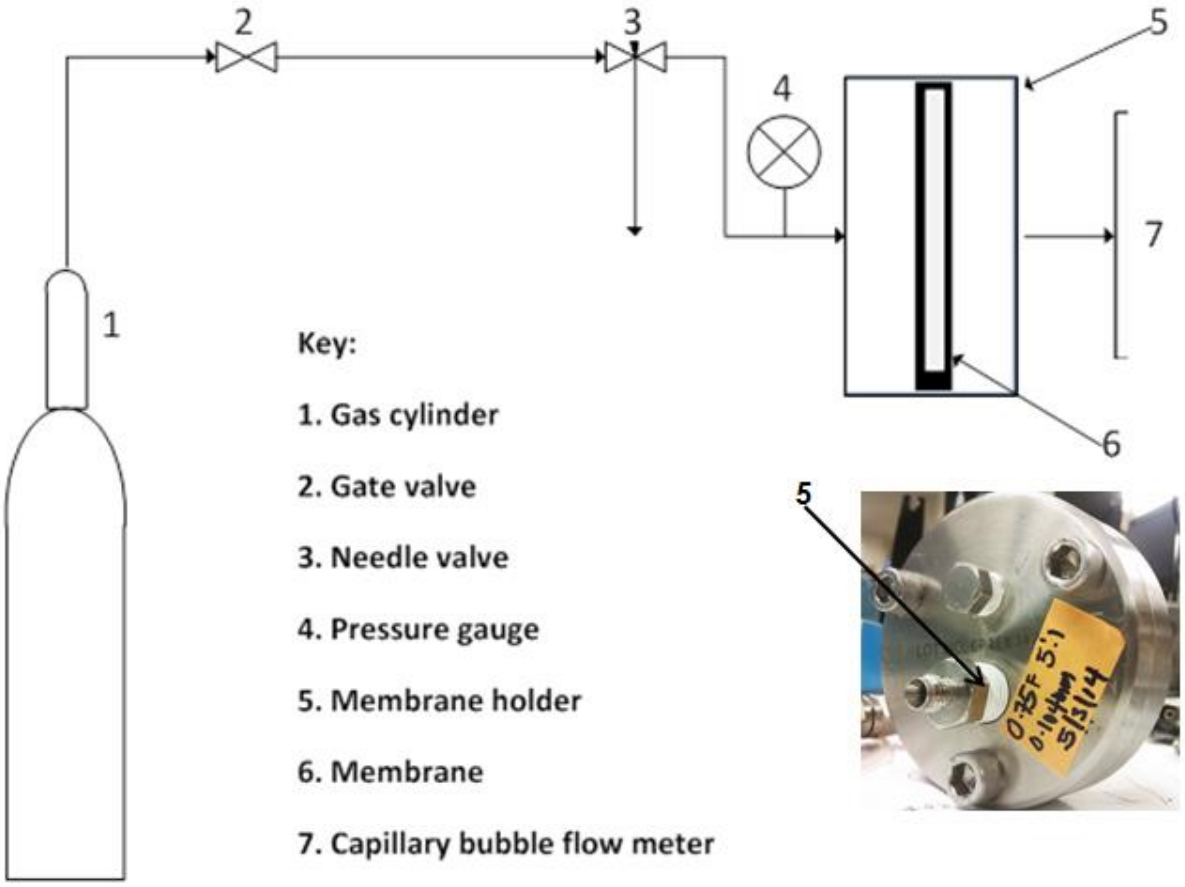

Figure 11. Schematic Laboratory Scale Set-up for Single Gas Permeation Test

CHAPTER 4

Results and Discussion

4.1 Fumed Silica and PDMS MMM Thermal Analysis

The thermal stability and degradation of the fumed silica (SiO_2), neat PDMS and SiO_2-PDMS were examined using TGA as shown on Figure 12.

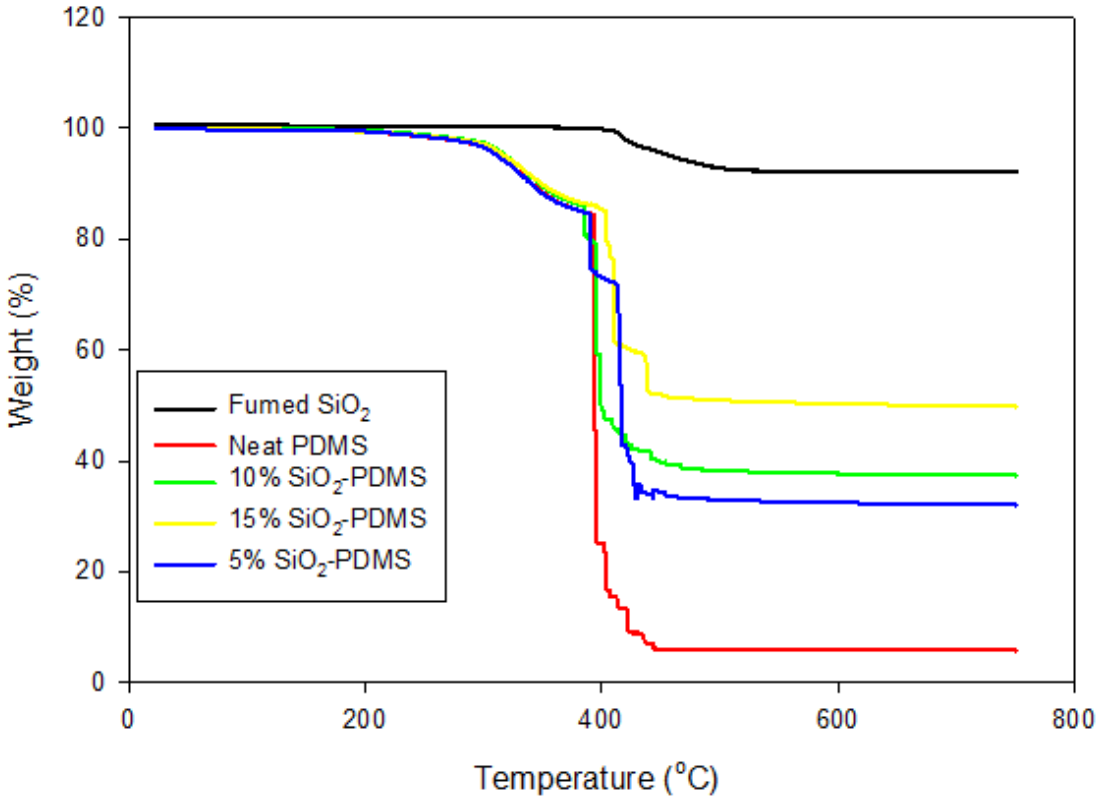

Figure 12. TGA Analysis of Fumed Silica, Neat PDMS and SiO_2-PDMS

The surface treated fumed silica had a total weight loss of 8.094% which may be attributed to the PDMS on SiO_2 surface and trace ambient contamination. Neat PDMS exhibited a significant weight loss of 94.20% with almost no char residue after the TGA test. This was due to the loss of methyl groups on the Si-O backbone [66]. The PDMS MMM with 5% wt, 10% wt,

and 15%wt silica loadings had 67.97%, 62.65, and 50.18% weight loss respectively as depicted on Figure 12 and Table 6.

Table 6

TGA Analysis of Fumed Silica, Neat PDMS and PDMS MMM

Sample	**Weight % loss**
Fumed Silica	8.09
Neat PDMS	94.20
5% SiO_2-PDMS	67.97
10% SiO_2-PDMS	62.65
15% SiO_2-PDMS	50.18

All the SiO_2-PDMS samples exhibited a similar degradation pattern to the neat PDMS in temperature range with degradation onset from between 200-325 ^{O}C and most abrupt at 400^{O}C. Ideally, the organic parts of the SiO_2-PDMS should be completely lost during the heating, leaving behind silica residue equal to silica weight percent added to PDMS matrix. However, all the SiO_2-PDMS samples had residues much higher than their respective silica contents (amount silica incorporated into the polymer matrix). This shows that the PDMS MMM did not totally degrade during the heating period because the silica had altered the thermal property of the polymer matrix. It is known that SiO_2 has superior heat insulation property and as fillers in PDMS, they can act as mass transport barriers by slowing down the release of produced volatile organics during thermal decomposition [48]. The higher residue weight (than the actual silica weight added to PDMS matrix), thus indicates a level of interaction between the polymer and silica chains and hence the improved thermal property (stability) of the PDMS MMM [67].

4.2 PDMS MMM Morphology

SEM analyses of the samples were carried out using Hitachi S-4800 field emission-scanning electron microscope. Samples were mounted on aluminum stubs with the help of two sided carbon tape. In order to avoid the charging, samples were coated with a thin layer of palladium.

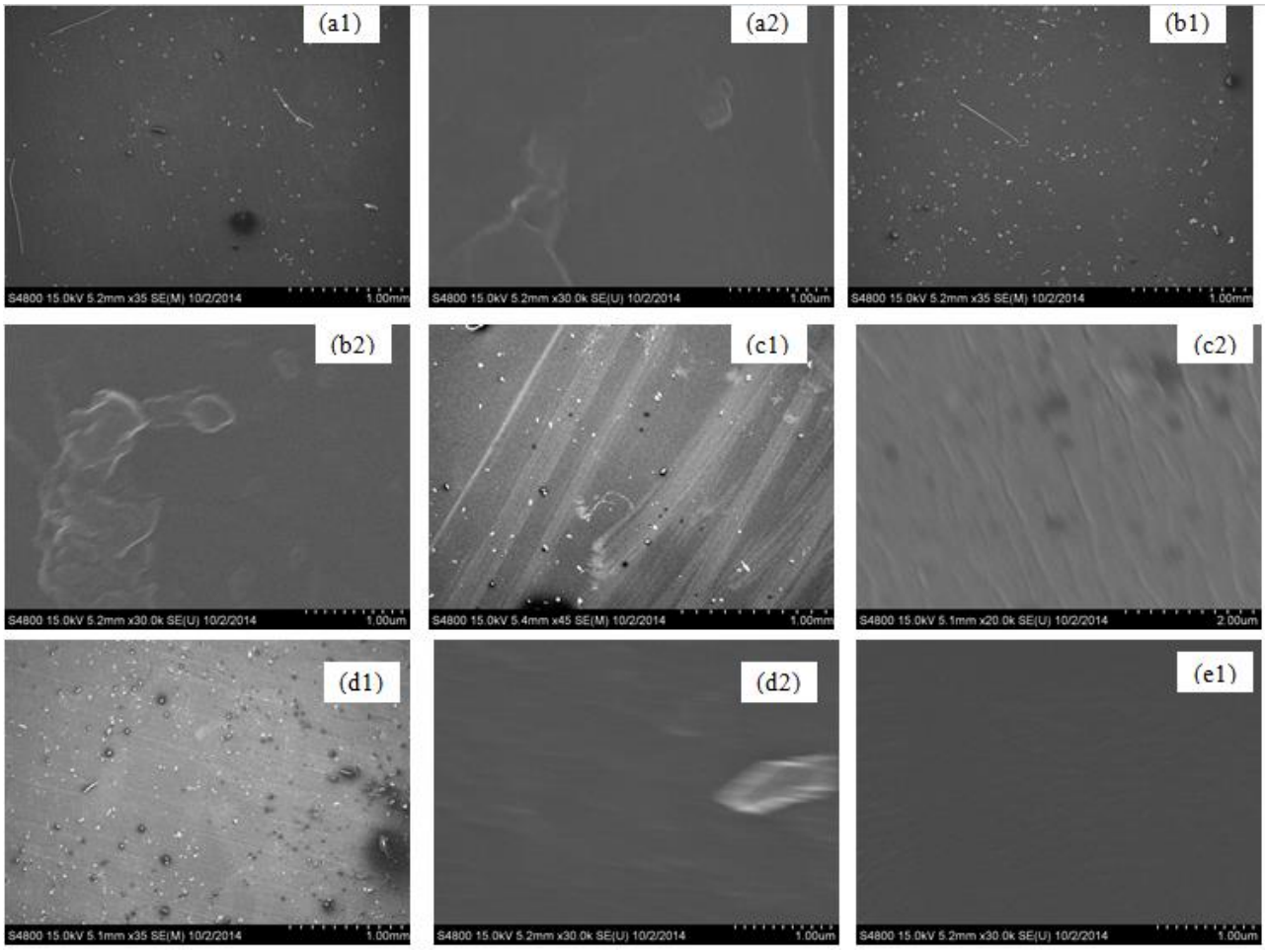

Figure 13. SEM Images of ($a_{1\&2}$) Neat PDMS X35&X30K; ($b_{1\&2}$) 5%SiO_2-PDMS X35 &X30k; ($c_{1\&2}$) 10%SiO_2-PDMS X35 & X30k; ($d_{1\&2}$) 15% SiO_2 PDMS X45 & 20K; (e1) 5% SiO_2 – PDMS-5 X30k

The dispersion of the surface-treated fumed silica in the PDMS matrix was investigated at different SEM magnifications (X35, X45, X20K and X30K). Figure 13a_1 and a_2 showed the surface and cross-section images of neat PDMS at X35 and X30K magnifications respectively. The surface images of the neat PDMS and the PDMS MMMs at X 35 and X45 on Figure 13. a_1 – d_1 all indicated the presence of dirt or dust (foreign) particles on the surface of membrane. The foreign particles could have settled on the membrane surface during solution casting and drying or must have been attracted during material handling (i.e. handling of membrane film). Foreign particles that got attracted to the surface of the membrane during material handling may not have any significant effect on the performance of the membrane; however, this depends on the nature of the particle. Dirt that settled on the surface of the viscous membrane solution after casting and through drying could affect the performance of the membrane. The cross-section images of all the composite membranes showed uniform distribution of the fumed silica; confirming good compatibility between the two phases. Good dispersion of the silica could be attributed to its hydrophobic nature and the silica surface treatment with PDMS as well as the laboratory procedure used in the synthesis of the membranes.

4.3 PDMS MMM Structure

In order to understand the structural effects of silica addition to PDMS matrix, FTIR spectra were recorded using Shimadzu IR Prestige-21 Fourier transform infrared (FTIR) 8300 spectrometer equipped with mercury-cadmium-telluride (MCD) detector as shown on fig.15. All the samples exhibited a moderate intensity peak at 2960 cm^{-1}. These bands correspond to the symmetric C-H bond stretching vibrations of the (CH_3) alkyl chains of the PDMS molecule. The absence of hydroxyl bond vibrations between 3200 cm^{-1} and 4000 cm^{-1} signified that all the

surface OH groups of the fume silica were consumed through bonding with the alkyl chains of the PDMS molecule. The absorption bands around 1257 cm^{-1} and 1012 cm^{-1} are attributed to the asymmetric stretching vibrations of Si-O-Si bonds. The intense peak between 788 cm^{-1} and 790 cm^{-1}could be attributed to the symmetric Si-O-Si bond vibrations [57].

No conspicuous spectral difference was observed when the silica loading was increased from 10% to 15%.

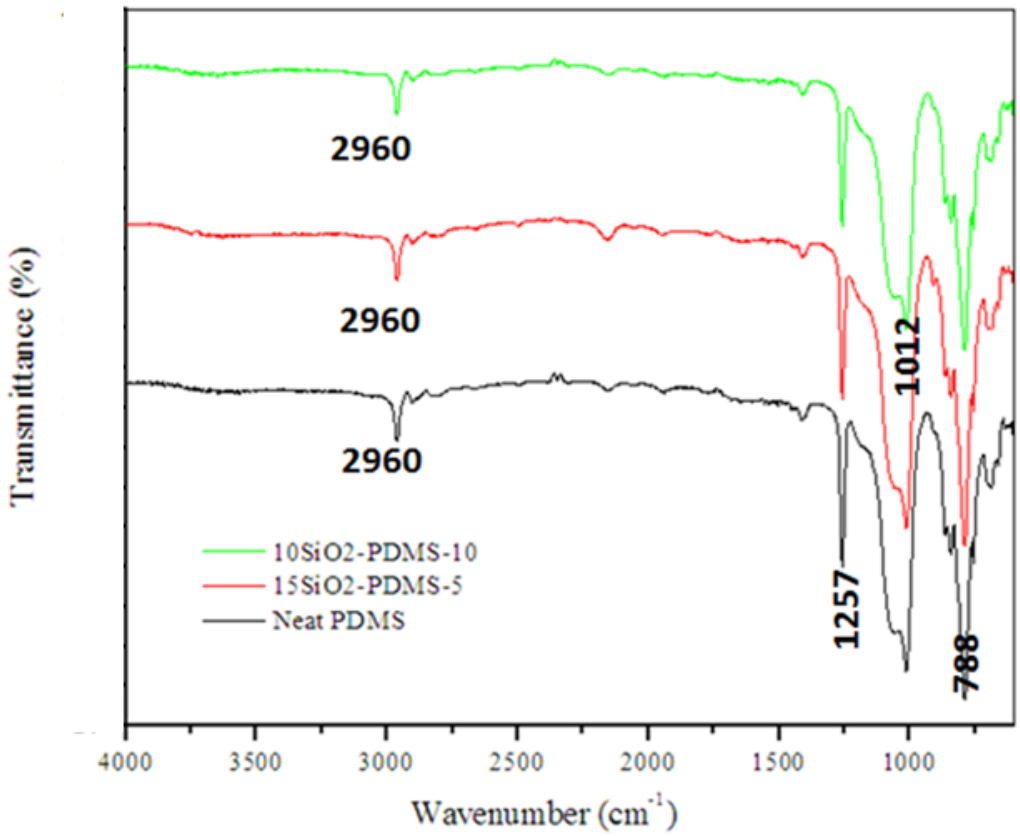

Figure 14. FTIR Spectra of Neat and PDMS MMM

4.4 Pure Gas Permeation Tests

4.4.1 Transport Pattern of O_2 and N_2 through Neat PDMS and 10%SiO_2-PDMS

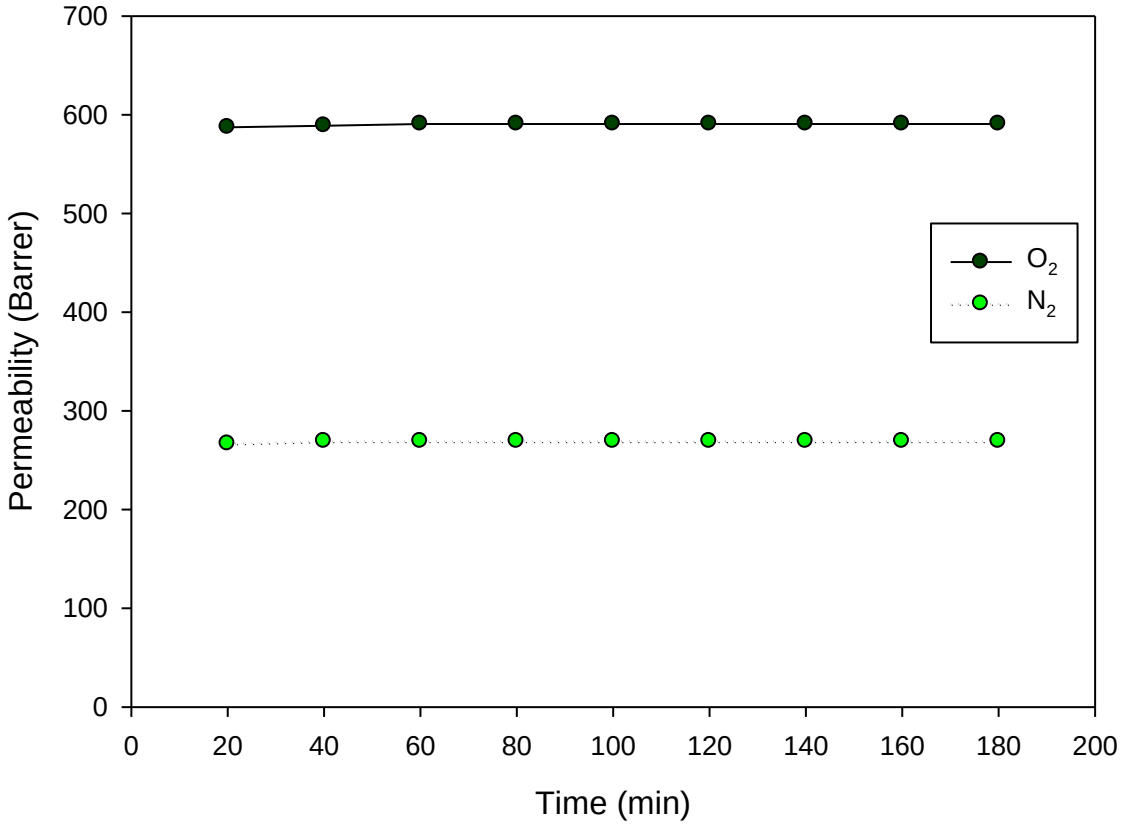

Figure 15. Transport Pattern of O_2 and N_2 through Neat PDMS membrane at 30 psig

The transport of O_2 and N_2 through neat PDMS membrane exhibited similar trend for both gases as shown on Figure 15; the gas flux (permeability) through the neat PDMS membrane increased slightly with time before attaining steady state flow rate. The incorporation of surface treated nano fumed silica into the PDMS matrix altered the N_2 flux pattern through the membrane as illustrated on Figure 16. Unlike the N_2 transport pattern observed in neat PDMS membrane, the gas (N_2) flux decreases with time before attaining steady state. The transport of O_2 through neat PDMS and PDMS MMM has the same pattern. Five PDMS MMMs with

different silica loading were subjected to gas permeation tests, all exhibited similar altered trend of N_2 flux observed on Figure 16.

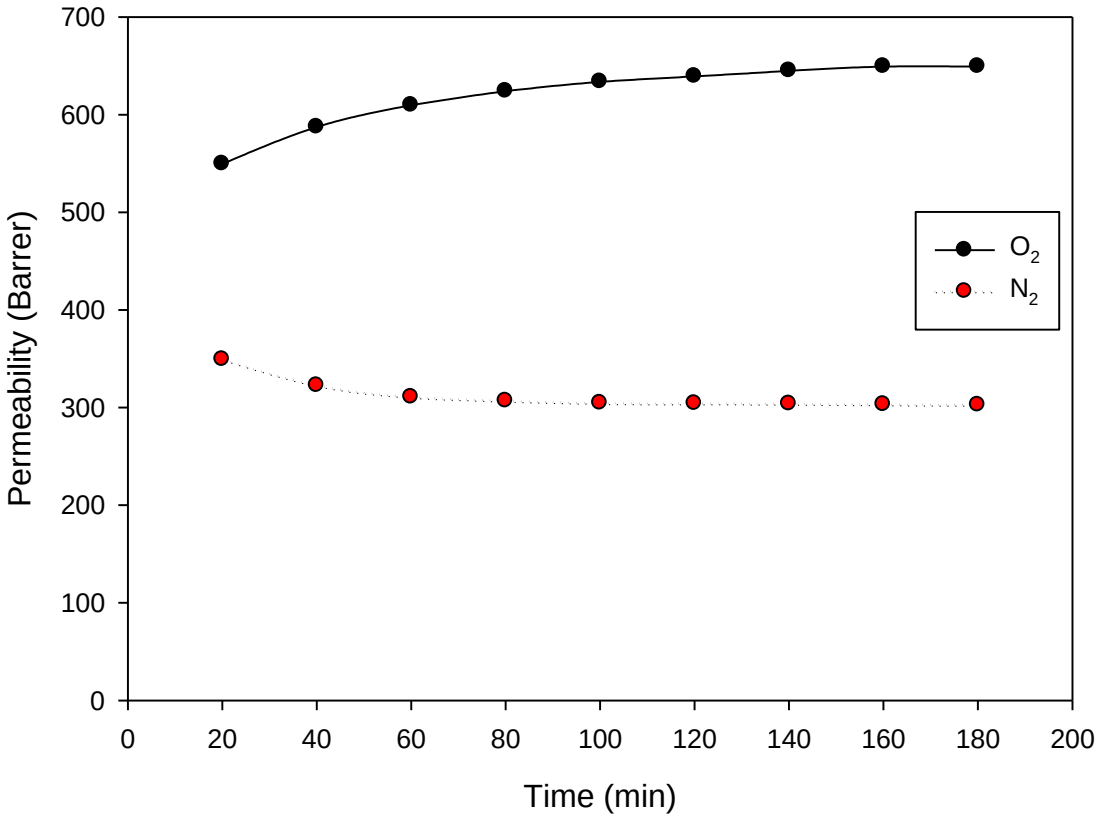

Figure 16. Transport Pattern of O_2 and N_2 through 10% SiO_2-PDMS at 30 psig

The incorporation of the silica altered the molecular packing of the polymer chains such that the transport of N_2 through it is affected. Goh and Ismail [28] reported that the addition of silica to polymer matrix gave rise to an increase in solubility and a corresponding decrease in the diffusivity of the gases through the MMMs, resulting in an enhanced permeability of more condensable gas (e.g. CO_2) in the polymer matrix and reduction in the permeability of the non-

condensable (e.g. N_2) gas, thereby changing the dominant gas permeation mechanism from diffusion to solution diffusion. They also pointed out that, the reduced diffusivity of the gases can be related to the restricted motion of the gas molecules in the polymer phase and formation of pathways with more tortuosity in the polymer upon the addition of silica particles. The altered transport pattern of N_2 through PDMS MMM on Figure 16 tends to confirm Goh and Ismail's report. So it can be concluded that the incorporation of fumed silica into PDMS matrix is responsible for the reduction of N_2 gas permeability with time before attaining steady state condition as observed in SiO_2-PDMS. Therefore, tailoring a SiO_2-PDMS with the ability to continuously and progressively slowdown the flux of N_2, while at the same time increasing the flux of O_2 for a long runtime before attaining steady state; this would result to an excellent membrane performance.

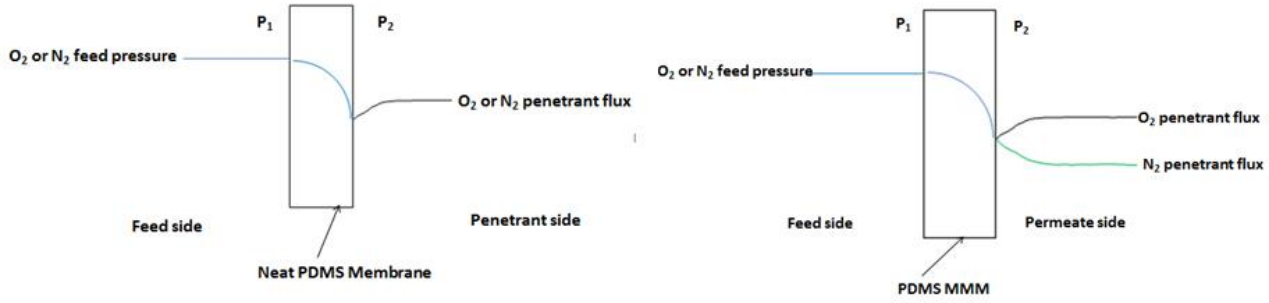

Figure 17. Transport Pattern of O_2/N_2 through Neat PDMS and SiO_2-PDMS

Figure 17. depicts the observed transport patterns of O_2 and N_2 through neat PDMS membrane and silica modulated PDMS membrane.

4.4.2 Effect of pure O_2 on PDMS MMM. To verify if continuous exposure of SiO_2-PDMS to O_2 has any effect on its stability, pure O_2 gas permeation test was conducted at 30 psig on a 10% SiO_2-PDMS MMM for 3hrs each day for three days as shown on Figure 18. Incorporation of silica is known to have significant effect on the molecular packing of the membrane and could affect its stability. As illustrated on Figure 18, the graphs of O_2 permeability for three days and other subsequent (similar) tests not included in this report superimposed each other; implying that the flux of O_2 through SiO_2-PDMS at the same operating condition with different runtimes remained the same. This shows that the PDMS MMM exposures to O_2 did not alter its property in terms of reactivity or stability wise.

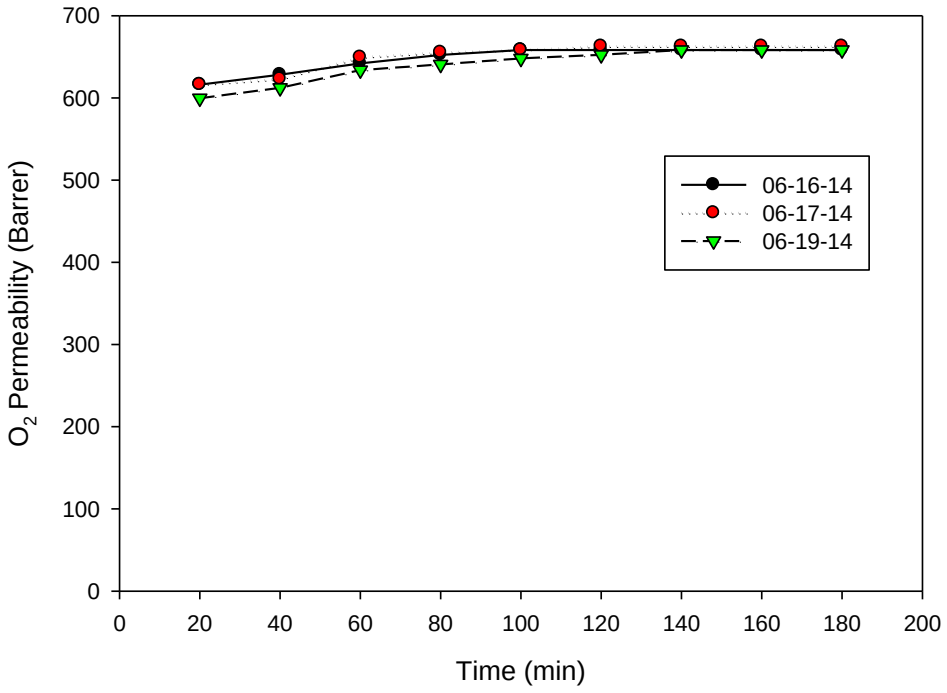

Figure 18. Effect of O_2 on PDMS MMM at 30 psi

4.4.3 Membrane performance for separation of O_2/N_2

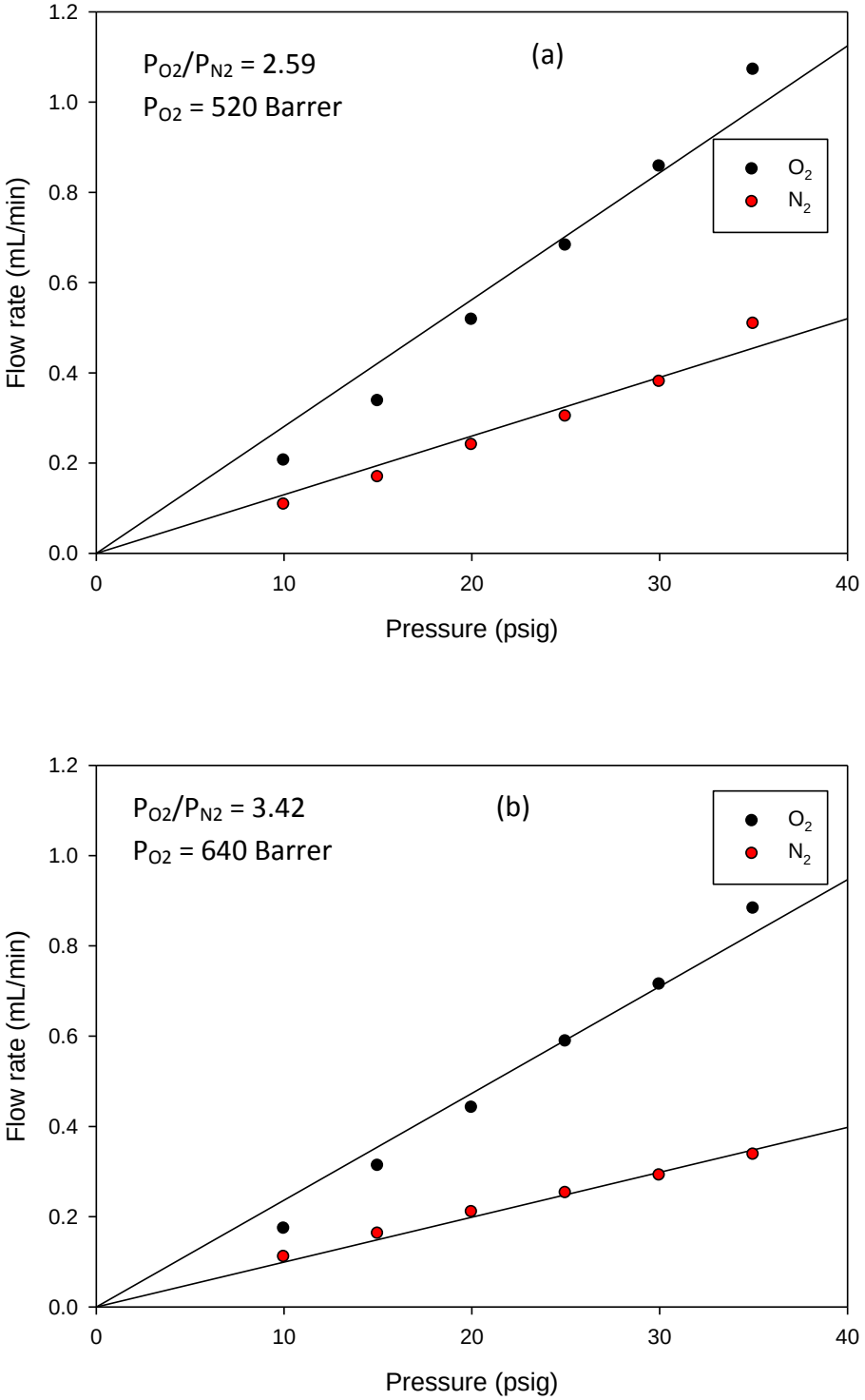

Figure 19: (a) Neat PDMS; (b) 10% SiO_2-PDMS Performance for O_2/N_2 Separation

Gas permeation tests on Figure 19a showed that the O_2 permeability for neat PDMS membrane was about 520 Barrer, with selectivity for O_2 over N_2 of 2.59. On the other hand, the 10% SiO_2-PDMS membrane not only exhibited much higher selectivity (3.42 for O_2), but also a higher O_2 permeability of 640 Barrer (Figure 19b.). The improved performance of the composite membrane could be attributed to the modified packing polymer matrix and phase separation of the membrane by the addition of the well dispersed silica nanoparticles in PDMS matrix.

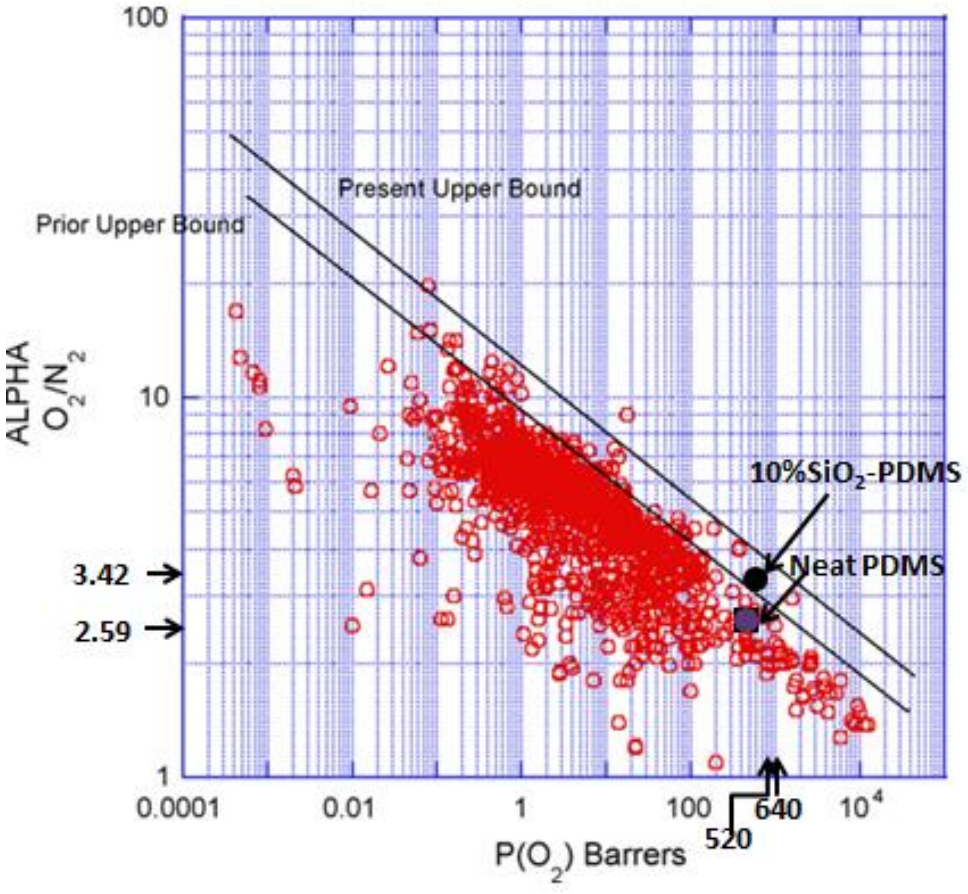

Figure 20. Upper Bound Correlation for O_2/N_2 Separation [63]

The L. Robeson's O_2/N_2 upper bound relationship has numerous data points that shows an intensity just below the original upper bound with a few data points emerging above allowing for a new upper bound relationship (Figure 20) [63]**.** Our 10% SiO_2-PDMS performance was slightly above the original upper bound but below the new upper bound. This indicates that the composite membrane has the potential to be commercialized should it possess all the other desirable properties of polymer membrane such as stability, reproducibility, processibility, low production cost, etc.

Table 7

Performances of Synthesized Neat PDMS and PDMS MMM

Membrane	***Crosslinking**	**PO_2 (Barrer)**	**Selectivity (O_2/N_2)**
Neat PDMS	10:1	520	2.59
5% SiO_2-PDMS	10:1	410	3.34
5% SiO_2-PDMS	5:1	517	3.28
10% SiO_2-PDMS	10:1	640	3.42
15% SiO_2-PDMS	10:1	521	2.76
15% SiO_2-PDMS	5:1	393	2.83
25% TEOS-PDMS [68]		370	3.45
15% SiO_2-PDMS [56]	10:1	-	2.50

** The term SiO_2-PDMS stands for membrane with 10:1 degree of crosslinking. When different degree of crosslinking is used other than 10:1, the ratio would be stated*.

The table above shows data for the performances of membranes under study; of all the membranes synthesized, 10% SiO_2-PDMS exhibited the best performance; others showed improvement over the neat PDMS.

4.4.4 Transport Pattern of CO_2 and CH_4 through Neat PDMS and 10%SiO_2-PDMS

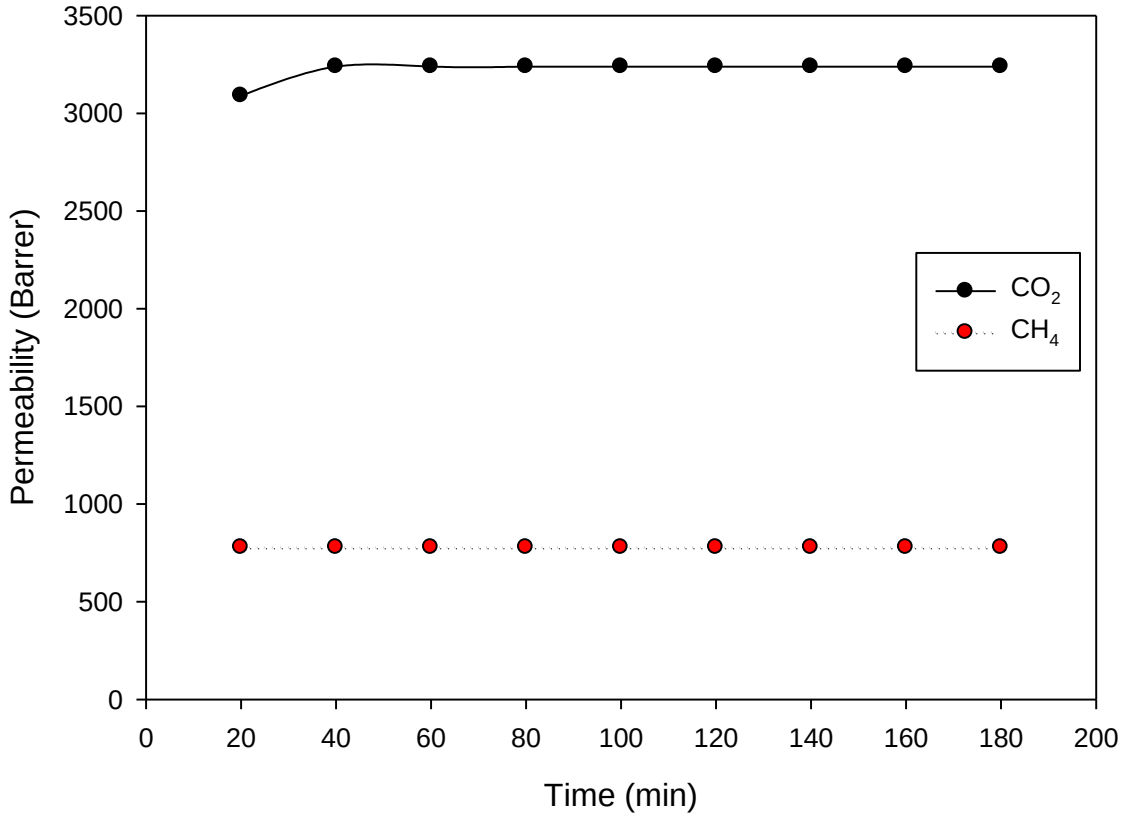

Figure 21. Transport Pattern of CO_2 and CH_4 through Neat PDMS at 15 psig

CO_2 and CH_4 have the same pattern of transport through unmodified PDMS. They both maintain constant fluxes through the membrane from the time the first gas permeation data were collected to the end of test (Figure 21). Both gases also maintain similar transport pattern through silica modified PDMS membrane. Figure 22 shows the graphs of CO_2 and CH_4 permeabilities, where both fluxes increased with time before attaining steady state. The incorporation of fumed silica in the polymer matrix as earlier discussed has the ability to alter the molecular packing of the polymer membrane chains. But then, this has no obvious benefit in comparison to its effects

on membrane performance when using O_2 and N_2 as a pair of gas as illustrated on Figure 16. Therefore, MMM (SiO_2-PDMS) does not have advantage over neat (PDMS) polymer membrane in CO_2/CH_4 separation.

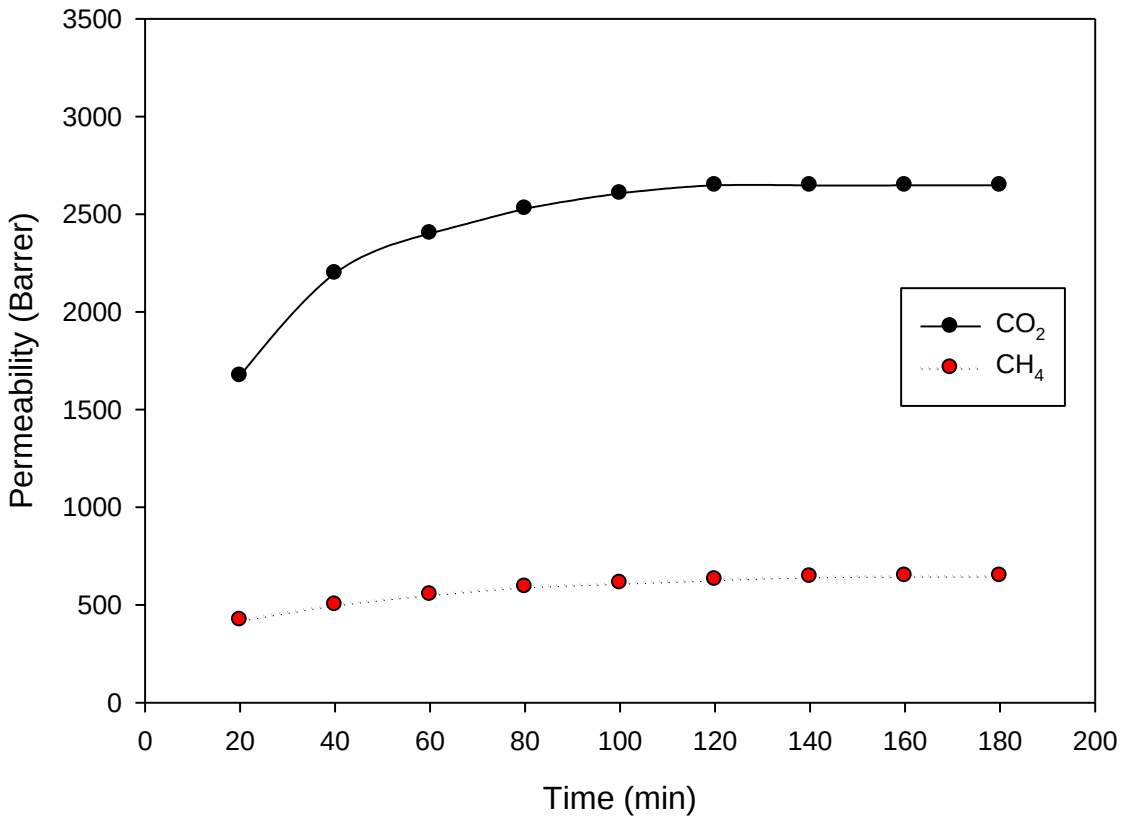

Figure 22. Transport Pattern of CO_2 and CH_4 through 10% SiO_2-PDMS at 15 psig

4.4.5 Pure gas permeabilities through neat PDMS and 10% SiO_2-PDMS

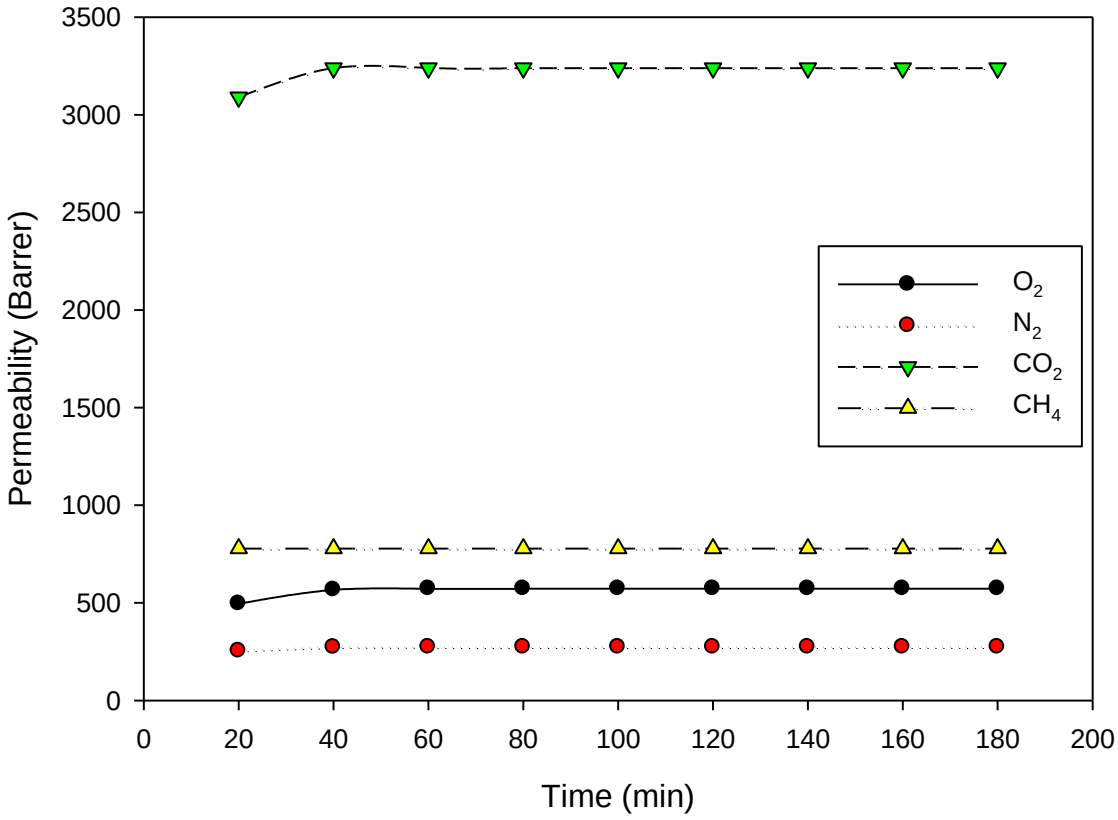

Figure 23. Pure Gas Permeabilities through Neat PDMS at 15 psig

Figures 23 and 24 illustrate the pure gas permeabilities of O_2, N_2, CO_2, and CH_4 in neat PDMS and 10% SiO_2-PDMS. The permeability values (for all the pure gases) from the neat PDMS membrane were similar to those found in literature [56]. However, the permeability values for CO_2 and CH_4 in 10% SiO_2-PDMS both decreased significantly relative to the values in the neat membrane but had almost the same selectivity as the neat PDMS shown on Figure 24. The neat and modified PDMS both have similar permeability trend of: $P_{CO2} > P_{CH4} > P_{O2} > P_{N2}$;

with corresponding penetrant gas critical temperatures (T_c) of 30.95^{0}C, -82.65^{0}C, -118.55^{0}C, and -146.55^{0}C [69].

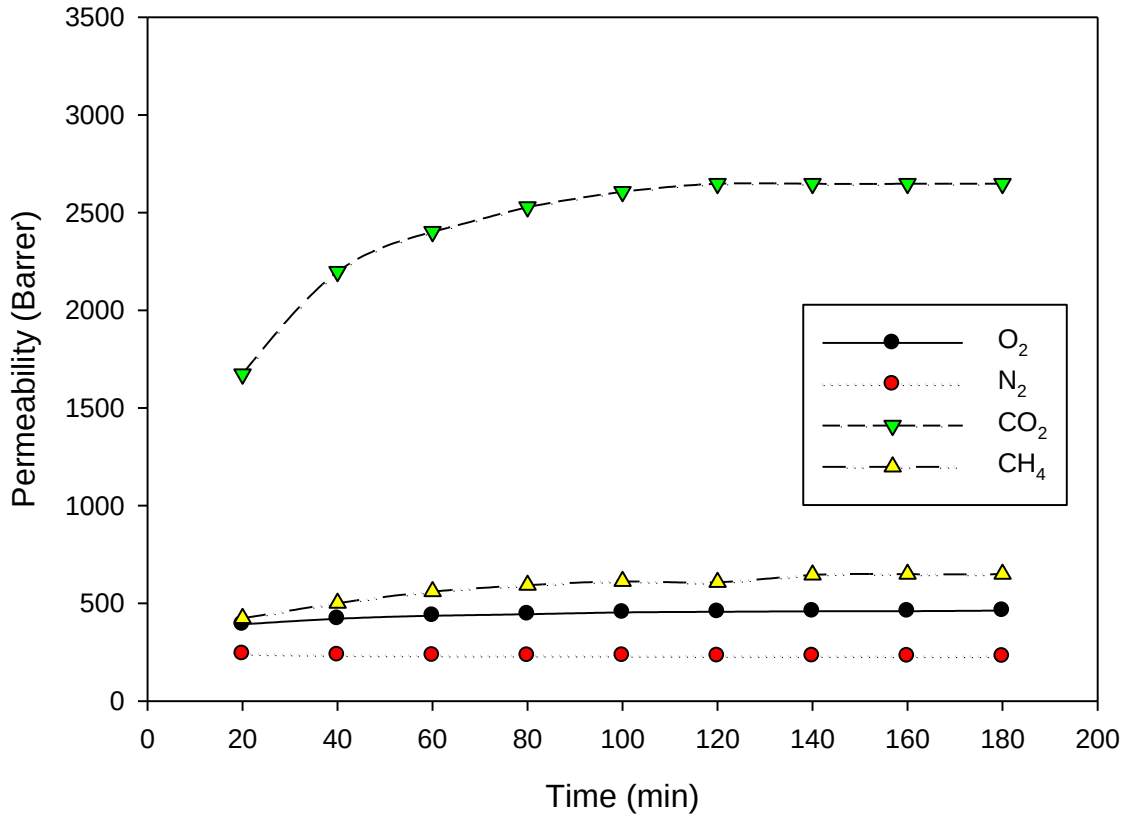

Figure 24. Pure Gas Permeabilities through 10% SiO_2-PDMS at 15 psig

For the two membranes, the permeabilities of CH_4 were much more than those N_2 and O_2 even with CH_4 having a the kinetic diameter (3.80 Å) greater than N_2 (3.64 Å) and O_2 (3.46Å). This could imply that gas solubility played more dominant role than diffusivity (gas molecule size dependent) in the transport of the penetrant gases through the membranes. Hence, higher Tc indicates higher gas condensability and therefore, higher solubility in the modified and unmodified membranes. Therefore, the permeability trend observed from the membranes is

typical for the tested gases since their relative permeabilities were mainly influenced by their relative solubilities [56].

4.4.6 Membrane Performance for separation of CO_2/CH_4

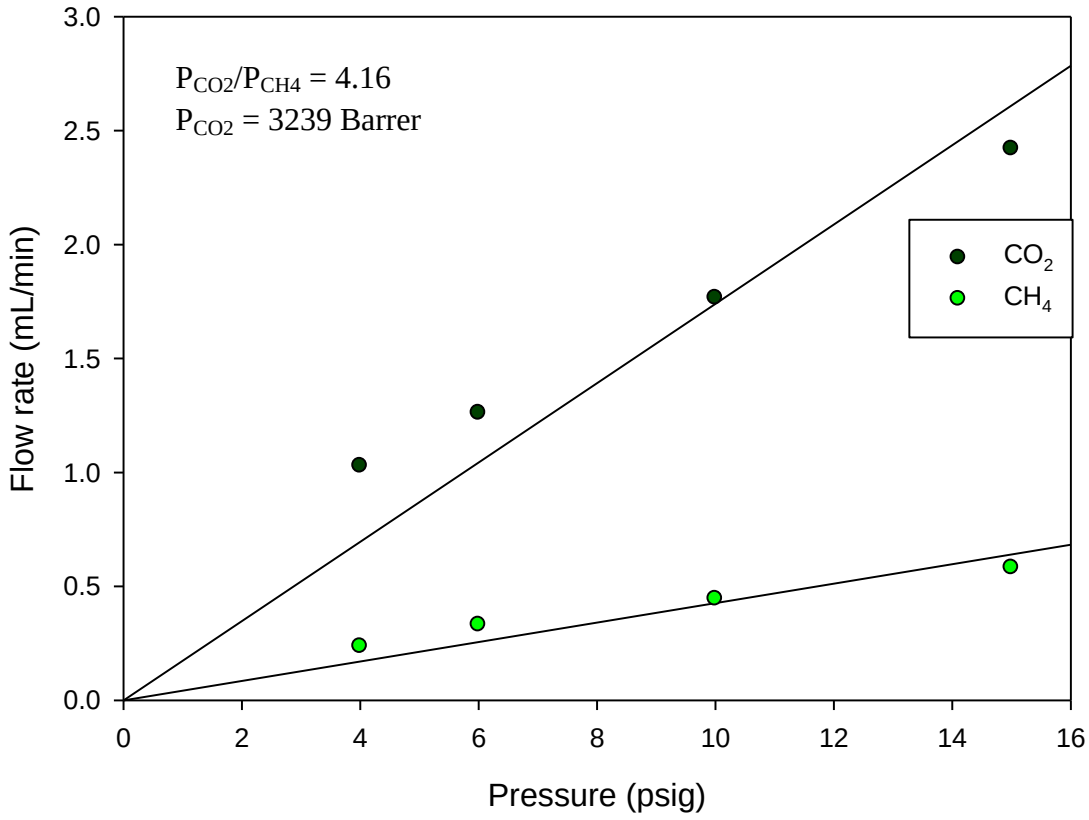

Figure 25. Neat PDMS Performance for CO_2/CH_4 Separation

Gas permeation tests on Figure 25 illustrates that the CO_2 permeability for neat PDMS membrane was about 3239 Barrer, with selectivity for CO_2 over CH_4 of 4.16. On the other hand, the 10% SiO_2-PDMS membrane exhibited a much lower permeability of 2967 Barrer with almost the same selectivity for CO_2 over CH_4 of 4.29 with the neat membrane (Figure 26). The CO_2 selectivities obtained from this study are higher than those reported in literatures [56, 69],

though they fall way below Robeson's upper bound correlation for CO_2/CH_4 separation (Figure 27).

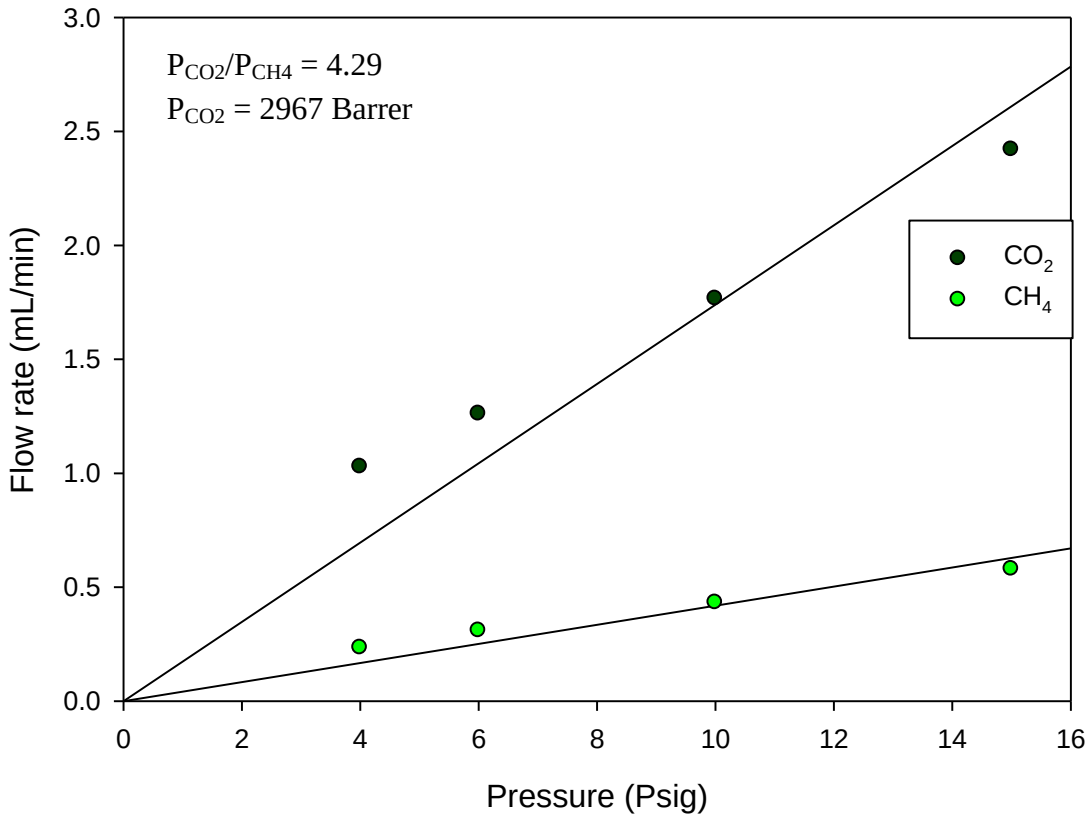

Figure 26. 10% SiO_2-PDMS Performance for CO_2/CH_4 Separation

The decline in the permeabilities of CO_2 and CH_4 in 10% SiO_2-PDMS could also be attributed to the modified packing patterns of the chains and morphology of the membrane as a result of the addition silica nanoparticles in PDMS matrix. The silica used for this study is obviously not suitable for membrane designed for separation of mixture of CO_2 and CH_4. Other fillers like zealot and carbon nanotubes could be more useful.

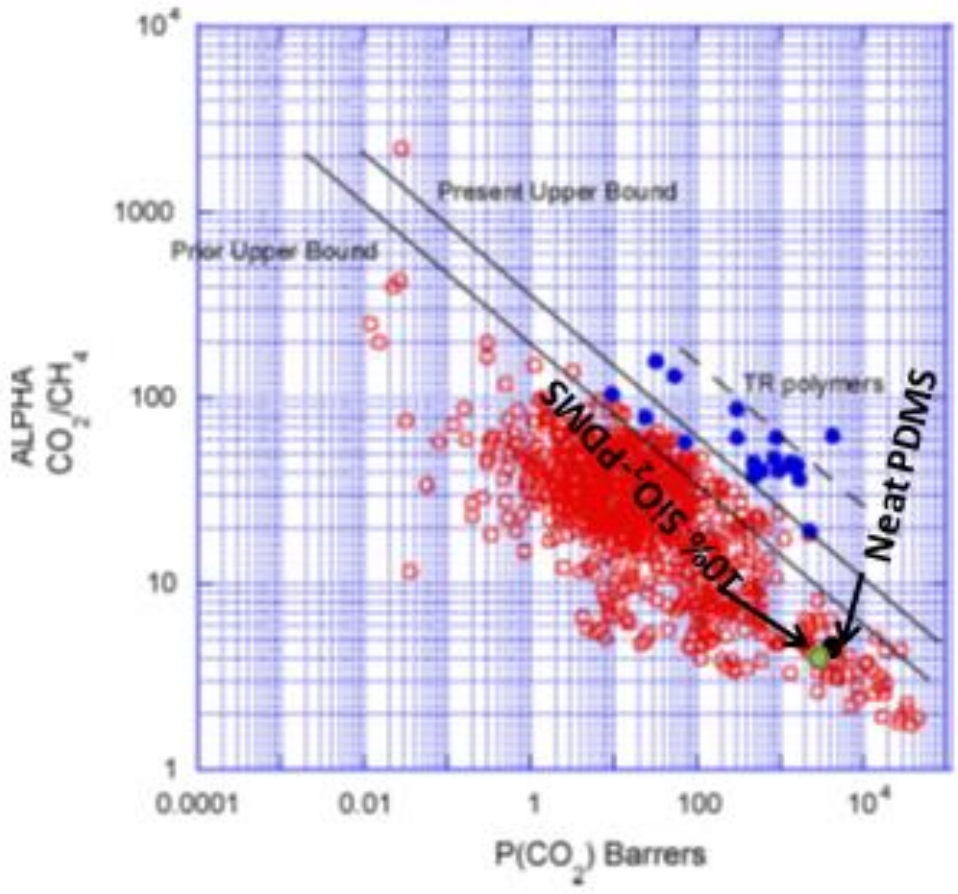

Figure 27. Upper bound Correlation for CO_2/CH_4 Separation

CHAPTER 5

Conclusions

Polydimethylsiloxane (PDMS) and surface-treated fumed silica were used to prepared mixed matrix membrane (SiO_2-PDMS) with different loadings of silica in the PDMS matrix. To enhance uniform dispersion and to avoid agglomeration of the nanosized silica particles in the membranes, toluene was used to control the viscosity of the polymer-silica solution. Techniques employed to characterize the synthesized neat PDMS and SiO_2-PDMS membrane confirmed good material compatibility between PDMS and fumed silica. SiO_2-PDMS exhibited an improved thermal property compared to neat PDMS. The presence of silica in the polymer enhanced the ease of material fabrication. The incorporation of surface treated nano fumed silica into the PDMS matrix altered the molecular packing of the polymer chains. The presences of silica in PDMS matrix changed the N_2 transport pattern through the membrane. Unlike the N_2 transport pattern observed in neat PDMS where the flux increased with time, N_2 flux through SiO_2-PDMS decreased with time before attaining steady state. The incorporation of silica into polymer matrix gave rise to an increase in solubility dominant flux and a corresponding decrease in the diffusivity of the gases through the MMMs. SiO_2-PDMS maintained stability under continuous and repeated exposure to O_2. 10% SiO_2-PDMS exhibited improved performance over neat PDMS for O_2/N_2 gas pair; whereas, neat PDMS had fair performance than 10% SiO_2-PDMS for the separation of CO_2/CH_4 gas pair. This implies that silica as nano filler in PDMS is not a suitable material for separation of CO_2/CH_4 gas pair. It could find useful application for CO_2/N_2 separation.

References

1. *Materials science of membranes for gas and vapor separation*, ed. I.P.a.B.F. Yuri Yampolskii. 2006, The Atrium, Southern Gate, Chichester, West Sussex PO19 8SQ, England: John Wiley & Sons Ltd,.
2. C., M.W.H.a.C.M., *Membranes for Natural Gas Sweetening and CO2 Enrichment.* Chemical Engineering Progress, 1982: p. 78.
3. Yi-Yan, N., R.M. Felder, and W.J. Koros, *Selective permeation of hydrocarbon gases in poly(tetrafluoroethylene) and poly(fluoroethylene–propylene) copolymer.* Journal of Applied Polymer Science, 1980. **25**(8): p. 1755-1774.
4. Fang, S.M., S.A. Stern, and H.L. Frisch, *A "free volume" model of permeation of gas and liquid mixtures through polymeric membranes.* Chemical Engineering Science, 1975. **30**(8): p. 773-780.
5. Freemantle, M., *Membranes for Gas Separation.* Chemical and Engineering News, 2005. **83**(40): p. 49-57.
6. Bastani, D., N. Esmaeili, and M. Asadollahi, *Polymeric mixed matrix membranes containing zeolites as a filler for gas separation applications: A review.* Journal of Industrial and Engineering Chemistry, 2013. **19**(2): p. 375-393.
7. Kim, S., et al., *Polysulfone and functionalized carbon nanotube mixed matrix membranes for gas separation: Theory and experiment.* Journal of Membrane Science, 2007. **294**(1–2): p. 147-158.

8. Burggraaf, A.J., *Chapter 2 Important characteristics of inorganic membranes*, in *Membrane Science and Technology*, A.J. Burggraaf and L. Cot, Editors. 1996, Elsevier. p. 21-34.

9. Smith, A.R. and J. Klosek, *A review of air separation technologies and their integration with energy conversion processes.* Fuel Processing Technology, 2001. **70**(2): p. 115-134.

10. Emsley, J., *Oxygen. In: Nature's building blocks: an A–Z guide to the elements,* 2011, Oxford, England (UK).

11. Leo, A., S. Liu, and J.C.D.d. Costa, *Development of mixed conducting membranes for clean coal energy delivery.* International Journal of Greenhouse Gas Control, 2009. **3**(4): p. 357-367.

12. Cengel Y, B.M., *Thermodynamics: an engineering approach*. 5 ed. 2006, New York: McGraw-Hill.

13. Moghadazadeh Zahra, T.J., and Mofarahi Masoud *Study of a Four-Bed Pressure Swing Adsorption for Oxygen Separation from Air* World Academy of Science, Engineering and Technology, 2008.

14. Yoshida, S., et al., *Study of Zeolite Molecular Sieves for Production of Oxygen by Using Pressure Swing Adsorption.* Adsorption, 1999. **5**(1): p. 57-61.

15. William J. Koros, R.T.C., *Handbook of separation process technology*, in *Separation of gaseous mixtures using polymer membrane* R.W. Rousseau, Editor 2014, A Wiley-lnterscience Publication: New York.

16. Robeson, L.M., *Polymer membranes for gas separation.* Current Opinion in Solid State and Materials Science, 1999. **4**(6): p. 549-552.

17. http://www.separationprocesses.com/Membrane/MT_Chp07a.htm, *Introduction to Membrane,* August 24, 2014.

18. Morooka S, K.K., *Microporous inorganic membranes for gas separation*, in *MRS Bulletin*1999, Cambridge Univ Press. p. 25-9.

19. Koresh JE, S.A., *Study of molecular sieve carbons. Part 2-Estimation of cross-sectional diameters of non-spherical molecules.* Journal of Chemical Society, 1980(76): p. 2472-80.

20. Zhang, Y., et al., *Current status and development of membranes for CO2/CH4 separation: A review.* International Journal of Greenhouse Gas Control, 2013. **12**(0): p. 84-107.

21. Reza Abedini, A.N., *Application of membrane in gas separation processes: Its suitability and mechanisms.* Petroluem and Coal, 2010(52(2)): p. 69-80.

22. Jiang, L.Y., et al., *Fundamental understanding of nano-sized zeolite distribution in the formation of the mixed matrix single- and dual-layer asymmetric hollow fiber membranes.* Journal of Membrane Science, 2005. **252**(1–2): p. 89-100.

23. Porter, M., *Handbook of Industrial Membrane Technology*. 1988, Park Ridge: Noyes Publications.

24. Robeson, L.M., *Correlation of separation factor versus permeability for polymeric membranes.* Journal of Membrane Science, 1991. **62**(2): p. 165-85.

25. Chung, T.-S., et al., *Mixed matrix membranes (MMMs) comprising organic polymers with dispersed inorganic fillers for gas separation.* Progress in Polymer Science, 2007. **32**(4): p. 483-507.

26. Caro J, N.M., Kolsch P, Scgaefer R., *Zeolite membrane-state of their development and perspective.* Microporous and Mesoporous Materials, 2000. **38**: p. 3-24.

27. Paul D.R. , K.D.R., *The diffusion time-lag in polymer membranes containing adsorption fillers 79–93.* Journal of Polymer Science, 1973. **41**: p. 79-93.

28. Goh, P.S., et al., *Recent advances of inorganic fillers in mixed matrix membrane for gas separation.* Separation and Purification Technology, 2011. **81**(3): p. 243-264.

29. Chung, T.-S., et al., *Characterization of permeability and sorption in Matrimid/C60 mixed matrix membranes.* Journal of Membrane Science, 2003. **211**(1): p. 91-99.

30. Lou, J.e.a., *Progress Report to DOE*, 2008.

31. Zimmerman, C.M., A. Singh, and W.J. Koros, *Tailoring mixed matrix composite membranes for gas separations.* Journal of Membrane Science, 1997. **137**(1–2): p. 145-154.

32. Şen, D., H. Kalıpçılar, and L. Yilmaz, *Development of polycarbonate based zeolite 4A filled mixed matrix gas separation membranes.* Journal of Membrane Science, 2007. **303**(1–2): p. 194-203.

33. Hashemifard, S.A., A.F. Ismail, and T. Matsuura, *Mixed matrix membrane incorporated with large pore size halloysite nanotubes (HNTs) as filler for gas separation: Morphological diagram.* Chemical Engineering Journal, 2011. **172**(1): p. 581-590.

34. Vu, D.Q., W.J. Koros, and S.J. Miller, *Mixed matrix membranes using carbon molecular sieves: I. Preparation and experimental results.* Journal of Membrane Science, 2003. **211**(2): p. 311-334.

35. Aroon, M.A., et al., *Performance studies of mixed matrix membranes for gas separation: A review.* Separation and Purification Technology, 2010. **75**(3): p. 229-242.

36. Moore, T.T., et al., *Hybrid membrane materials comprising organic polymers with rigid dispersed phases.* AIChE Journal, 2004. **50**(2): p. 311-321.

37. S. Bertelle, T.G., D. Roizard, C. Vallières, E. Favre, , *Study of polymer–carbon mixed matrix membranes for CO2 separation from flue gas* Desalination 2006. **199**: p. 401-402.

38. Ahn, J., et al., *Polysulfone/silica nanoparticle mixed-matrix membranes for gas separation.* Journal of Membrane Science, 2008. **314**(1–2): p. 123-133.

39. Cong, H., et al., *Polymer–inorganic nanocomposite membranes for gas separation.* Separation and Purification Technology, 2007. **55**(3): p. 281-291.

40. Mahajan, R. and W.J. Koros, *Mixed matrix membrane materials with glassy polymers. Part 2.* Polymer Engineering & Science, 2002. **42**(7): p. 1432-1441.

41. Anson, M., et al., *ABS copolymer-activated carbon mixed matrix membranes for CO_2/CH_4 separation.* Journal of Membrane Science, 2004. **243**(1–2): p. 19-28.

42. Moaddeb, M. and W.J. Koros, *Gas transport properties of thin polymeric membranes in the presence of silicon dioxide particles.* Journal of Membrane Science, 1997. **125**(1): p. 143-163.

43. Hu, Q., et al., *Poly(amide-imide)/TiO2 nano-composite gas separation membranes: Fabrication and characterization.* Journal of Membrane Science, 1997. **135**(1): p. 65-79.

44. Bernardo, P., E. Drioli, and G. Golemme, *Membrane Gas Separation: A Review/State of the Art.* Industrial & Engineering Chemistry Research, 2009. **48**(10): p. 4638-4663.

45. Ghadimi, A., M. Sadrzadeh, and T. Mohammadi, *Prediction of ternary gas permeation through synthesized PDMS membranes by using Principal Component Analysis (PCA) and fuzzy logic (FL).* Journal of Membrane Science, 2010. **360**(1–2): p. 509-521.

46. Messori, M., *In Situ Synthesis of Rubber Nanocomposites*, in *Recent Advances in Elastomeric Nanocomposites*, V. Mittal, J.K. Kim, and K. Pal, Editors. 2011, Springer Berlin Heidelberg. p. 57-85.

47. Paola Bernardo*, G.C.a.J.C.J., *Silicone Membranes for Gas, Vapor and Liquid Phase Separations*, in *Concise Encyclopedia of High Performance Silicones*, A.T. and and M.D. Soucek, Editors. 2014, Scrivener Publishing: 100 Cummings Center, Suite 541J Beverly, MA 01915-6106. p. 309-318.

48. Hua Zou, S.W., and Jian Shen, *Polymer/Silica Nanocomposites: Preparation, Characterization, Properties, and Applications* Chemical Review, 2008. **108**: p. 3893-3957.

49. Gomes, D., S.P. Nunes, and K.-V. Peinemann, *Membranes for gas separation based on poly(1-trimethylsilyl-1-propyne)–silica nanocomposites.* Journal of Membrane Science, 2005. **246**(1): p. 13-25.

50. Kim, J.H. and Y.M. Lee, *Gas permeation properties of poly(amide-6-b-ethylene oxide)–silica hybrid membranes.* Journal of Membrane Science, 2001. **193**(2): p. 209-225.

51. Koros, W.J. and G.K. Fleming, *Membrane-based gas separation.* Journal of Membrane Science, 1993. **83**(1): p. 1-80.

52. Merkel, T.C., et al., *Ultrapermeable, Reverse-Selective Nanocomposite Membranes.* Science, 2002. **296**(5567): p. 519-522.

53. Morisato, A., et al., *Transport properties of PA12-PTMO/AgBF4 solid polymer electrolyte membranes for olefin/paraffin separation.* Desalination, 2002. **145**(1–3): p. 347-351.

54. Gao Y., C.N.R., *Gao, Y.; Choudhury, N. R. In Handbook of Organic-Inorganic Hybrid Materials and Nanocomposites*. Vol. 1. 2003, Stevenson Ranch: Nalwa, H. S., Ed.; American Scientific Publishers.

55. Nelson, J.K.M., R.K. ; Schadler, L.S, *Polymer nanocomposite dielectrics-the role of the interface.* Dielectric Electrical Insulation, IEEE Transactions, 2005. **12**(4): p. 629.

56. etal, G.M.N.A.B.B., *Dimethyl silane-modified silica in polydimethylsiloxane as gas permeation mixed matrix membrane.* Journal of Polymer Resources, 2011. **12**: p. 2415-2424.

57. J., E.K.W.W.G., *Surface modificationof Sylgard-184 poly(dimethyl siloxane) networks by ultraviolet and ultraviolet/ozone treatment.* . Journal Colloid Interface Science and Technology of Advanced Materials, 2002. **254**: p. 306–315.

58. Y., B. and 97:402–408, *UV/ozone modification of poly(dimethylsiloxane) microfluidic channels.* Sensor Actuat B-Chem, 2004.

59. Hierold C, B.O., Fedder G.; Korvink J., *Carbon Nanotube Devices: Properties, Modeling, Integration and Applications*. 2008: Wiley-VCH.

60. Liu, Y.-L., C.-Y. Hsu, and K.-Y. Hsu, *Poly(methylmethacrylate)-silica nanocomposites films from surface-functionalized silica nanoparticles.* Polymer, 2005. **46**(6): p. 1851-1856.

61. Schild, H.G., *Poly(N-isopropylacrylamide): experiment, theory and application.* Progress in Polymer Science, 1992. **17**(2): p. 163-249.

62. Schow, A.J., R.T. Peterson, and J.D. Lamb, *Polymer inclusion membranes containing macrocyclic carriers for use in cation separations.* Journal of Membrane Science, 1996. **111**(2): p. 291-295.

63. Robeson, L.M., *The upper bound revisited.* Journal of Membrane Science, 2008. **320**(1–2): p. 390-400.

64. http://www.oit.doe.gov. *Oxygen Enriched Combustion*. 2005.

65. www.airliquide.com. *Oxygen applications*. 2014.

66. Jovanovic, J.D., et al., *The thermogravimetric analysis of some polysiloxanes.* Polymer Degradation and Stability, 1998. **61**(1): p. 87-93.

67. Krishnamachari, P., et al., *Biodegradable Poly(Lactic Acid)/Clay Nanocomposites by Melt Intercalation: A Study of Morphological, Thermal, and Mechanical Properties.* International Journal of Polymer Analysis and Characterization, 2009. **14**(4): p. 336-350.

68. Rao, H.-X., F.-N. Liu, and Z.-Y. Zhang, *Preparation and oxygen/nitrogen permeability of PDMS crosslinked membrane and PDMS/tetraethoxysilicone hybrid membrane.* Journal of Membrane Science, 2007. **303**(1–2): p. 132-139.

69. José, N.M., L.A.S.A. Prado, and I.V.P. Yoshida, *Synthesis, characterization, and permeability evaluation of hybrid organic–inorganic films.* Journal of Polymer Science Part B: Polymer Physics, 2004. **42**(23): p. 4281-4292.